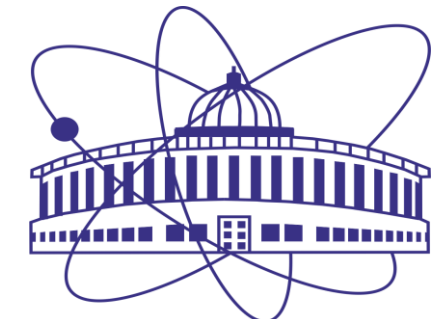
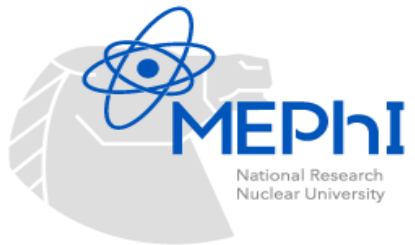


System Size/Rapidity Scan - MPD

Arkadiy Taranenko
(NRNU MEPhI, JINR)



15th MPD Collaboration Meeting
15-17 April 2025, JINR

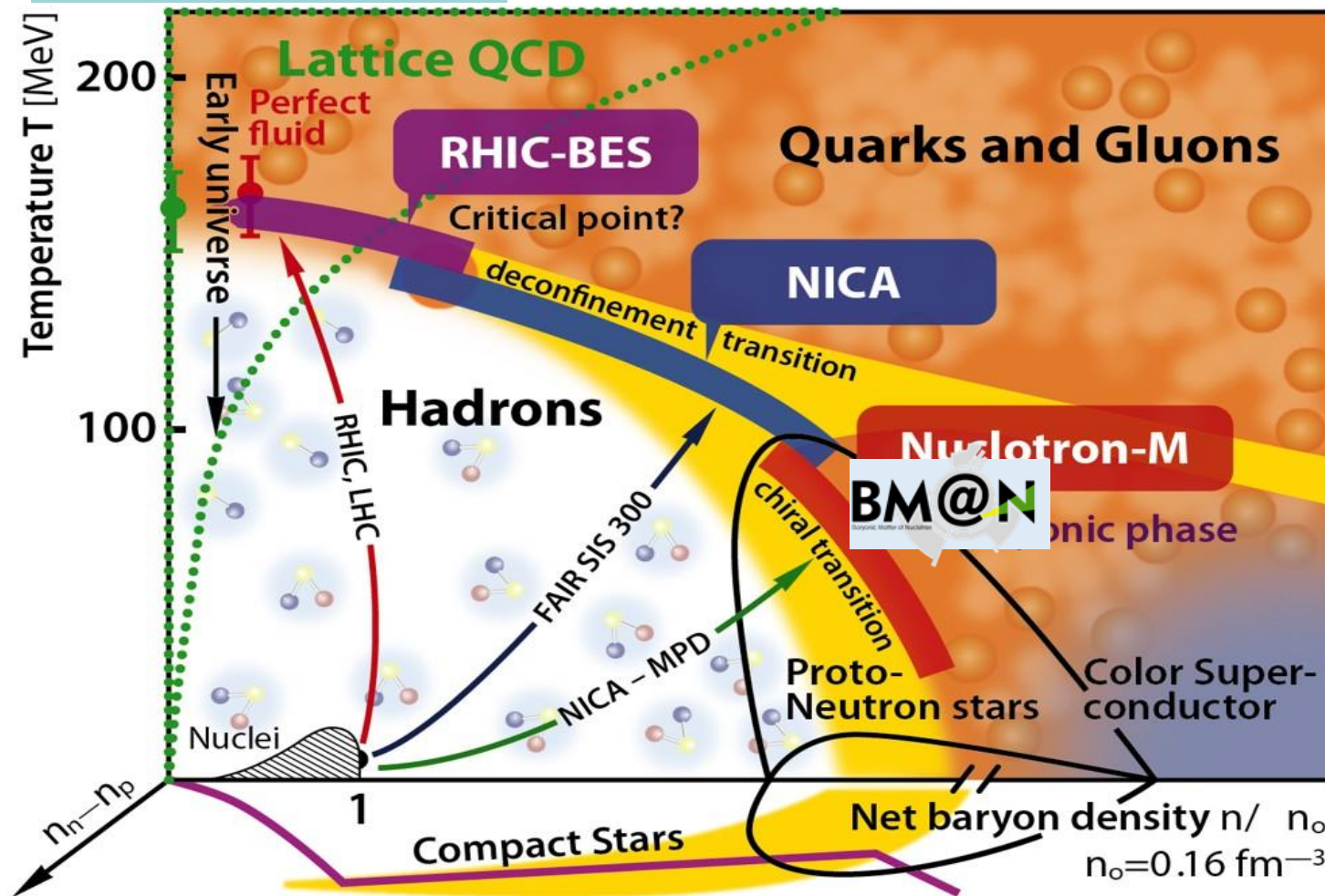


Relativistic Heavy-Ion Collisions and QCD Phase Diagram

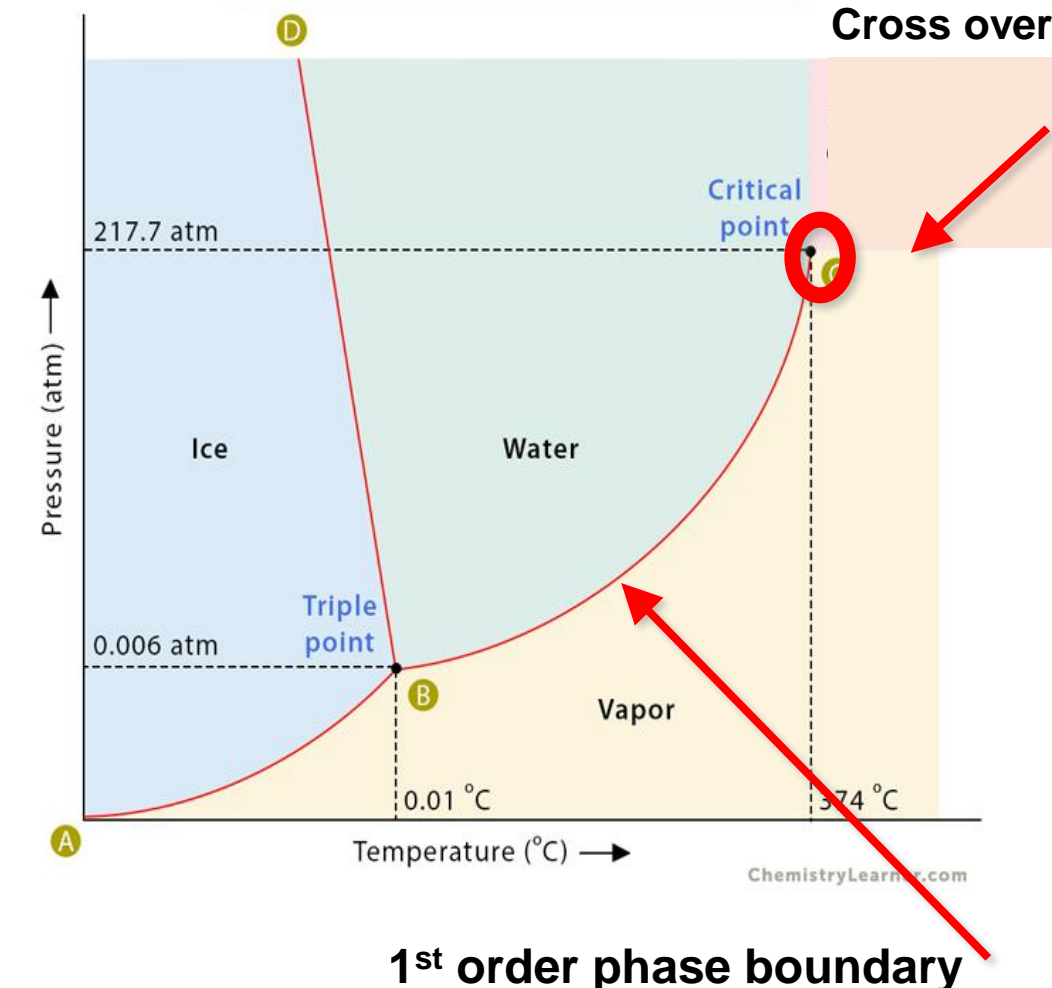
Critical Temperature

$$T_c \approx 156 \pm 9 \text{ MeV}$$

[PRD 90 094503 (2014)]

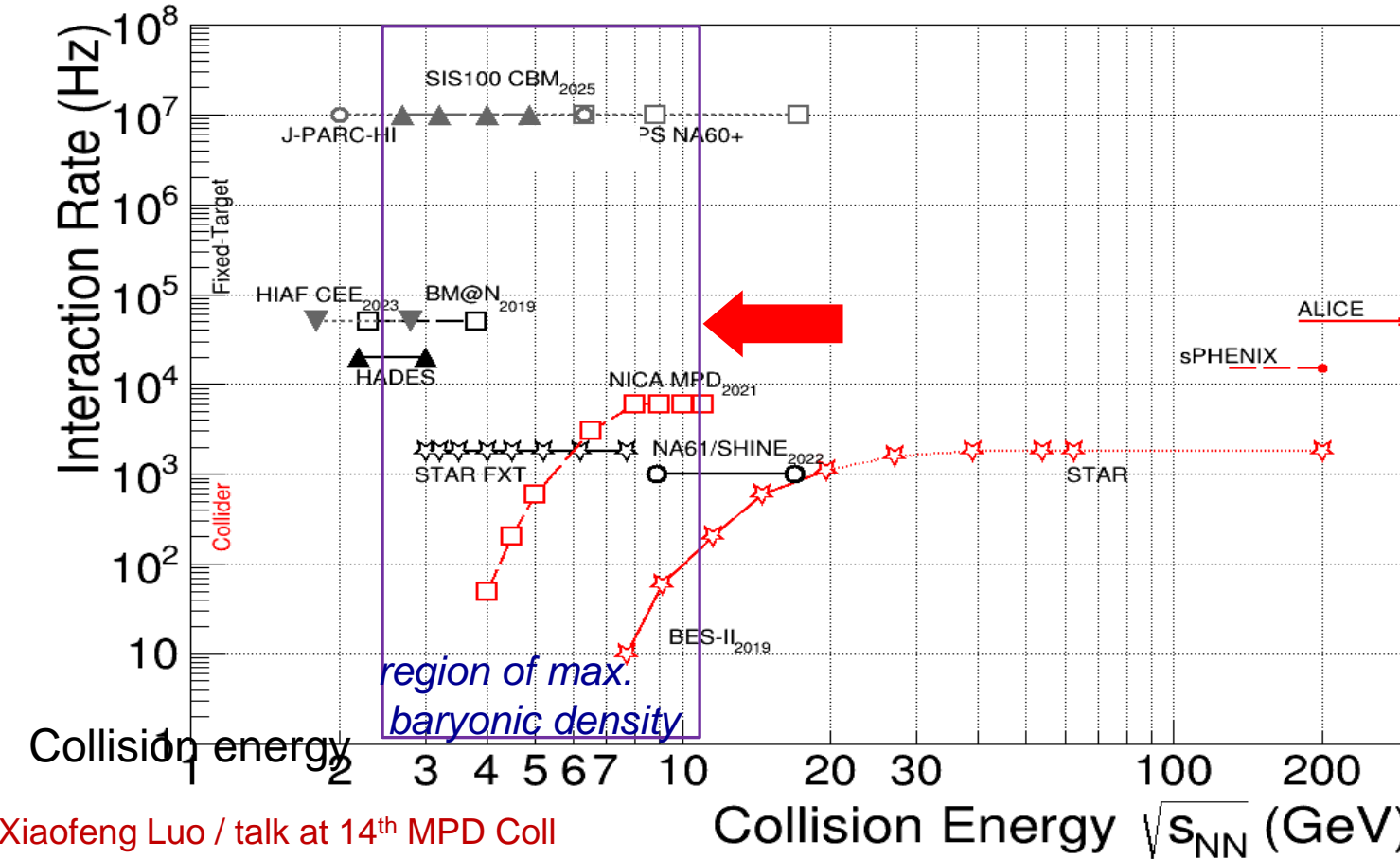


Phase Diagram of Water



Smooth transition from hadronic degrees of freedom to quark-gluon degrees of freedom at zero baryonic density

Relativistic Heavy Ion Collision Experiments



Method	μ_c (MeV)	T_c (MeV)
Holography + Bayesian	560 - 625	101 - 108
FRG/DSE	495 - 654	108 - 119
Lee-Yang edge singularities	500 - 600	100 - 105
Lattice QCD	$\mu_c/T_c > 3$	F. Karsch et al.
Summary	495 - 654	100 - 119

$$(\mu_c, T_c) = (495 - 654, 100 - 119) \text{ MeV} \rightarrow 3.5 < \sqrt{s_{NN}} < 4.9 \text{ GeV}$$

MPD competitors:

Present:

RHIC/STAR (USA) 3-200 GeV
SPS/NA61 (CERN) 5.1-17.3 GeV

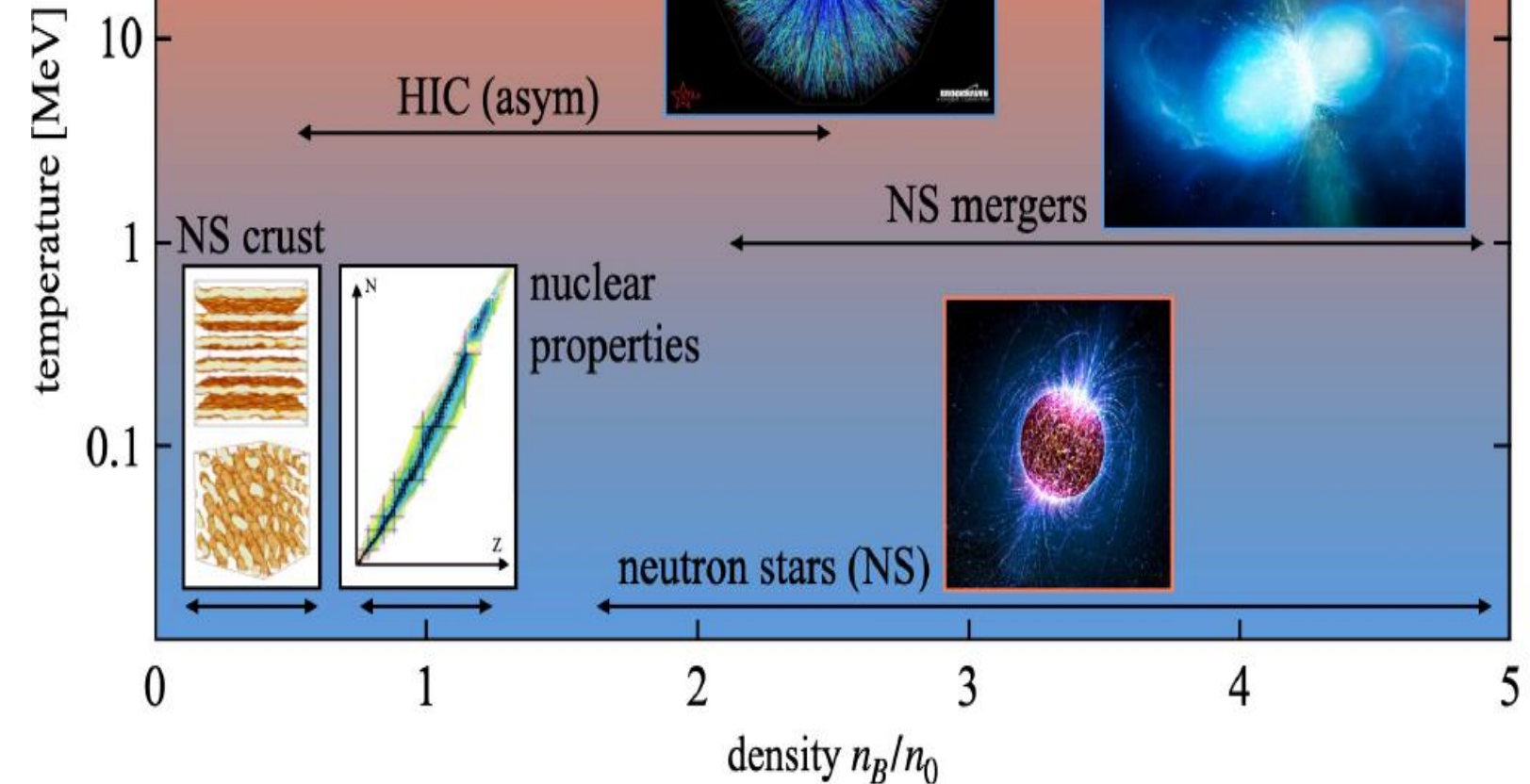
Future:

HIAF/CEE (China) 2.1-4.5 GeV (2026-?)
FAIR/CBM (Germany) 2.4-4.9 GeV (2029-?)
JPARC-HI (Japan) 2-5 GeV (2030-?)

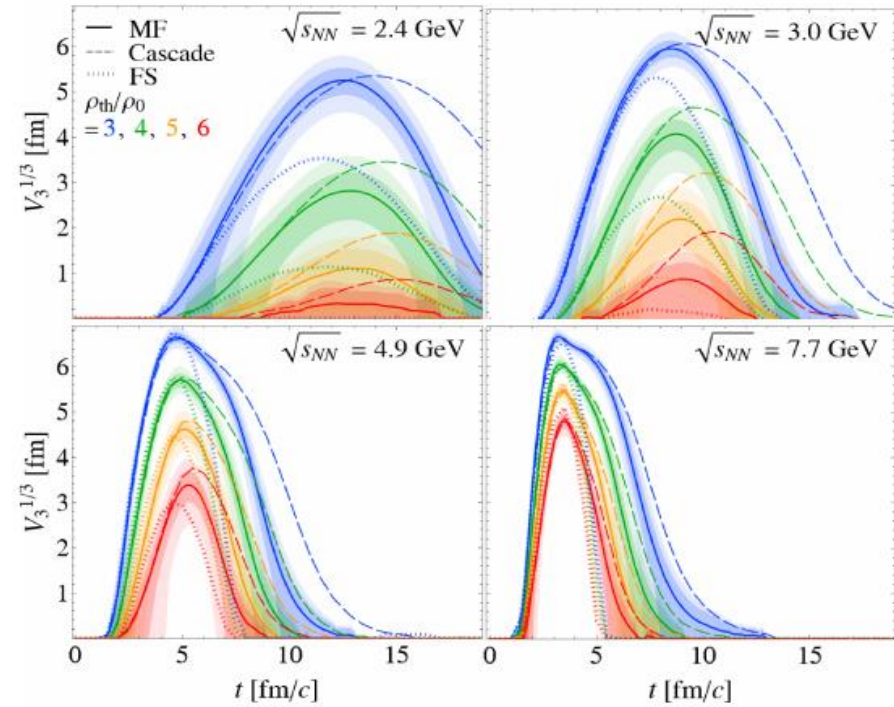
BM@N: $\sqrt{s_{NN}} = 2.3 - 3.3 \text{ GeV}$
MPD: $\sqrt{s_{NN}} = 4 - 11 \text{ GeV}$

BM@N and MPD are both in the collision energy range of the predicted CEP location.

Dense Nuclear Matter



J.Subatomic Part.Cosmol. 3 (2025) 100015



Relativistic heavy-ion collisions provide a unique and controlled experimental way to study the properties of nuclear matter at high baryon density.

Equation of state (EoS) for high baryon density matter

pressure

$$P = n^2 \frac{d(E/A)}{dn_b}$$

energy per nucleon

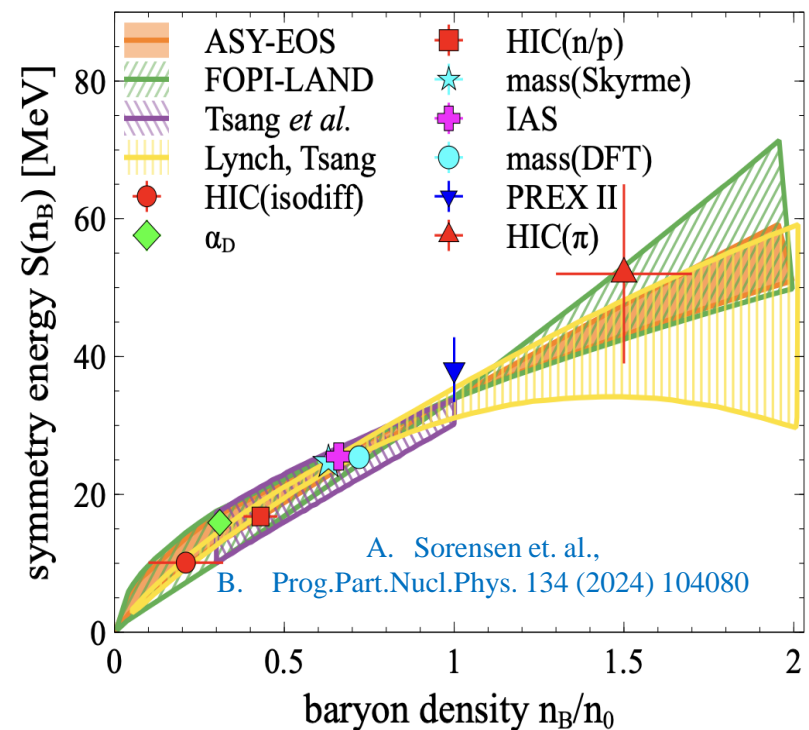
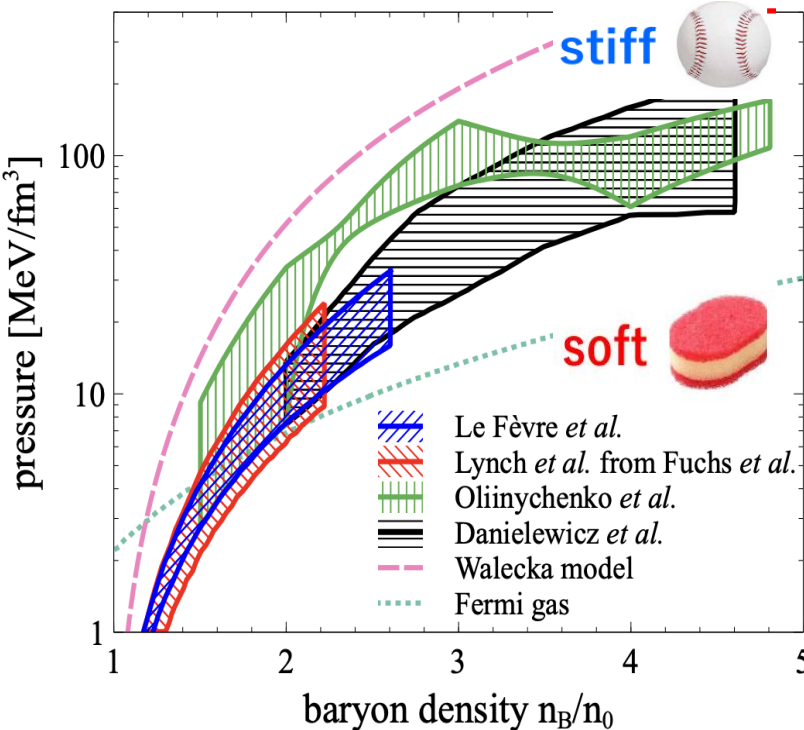
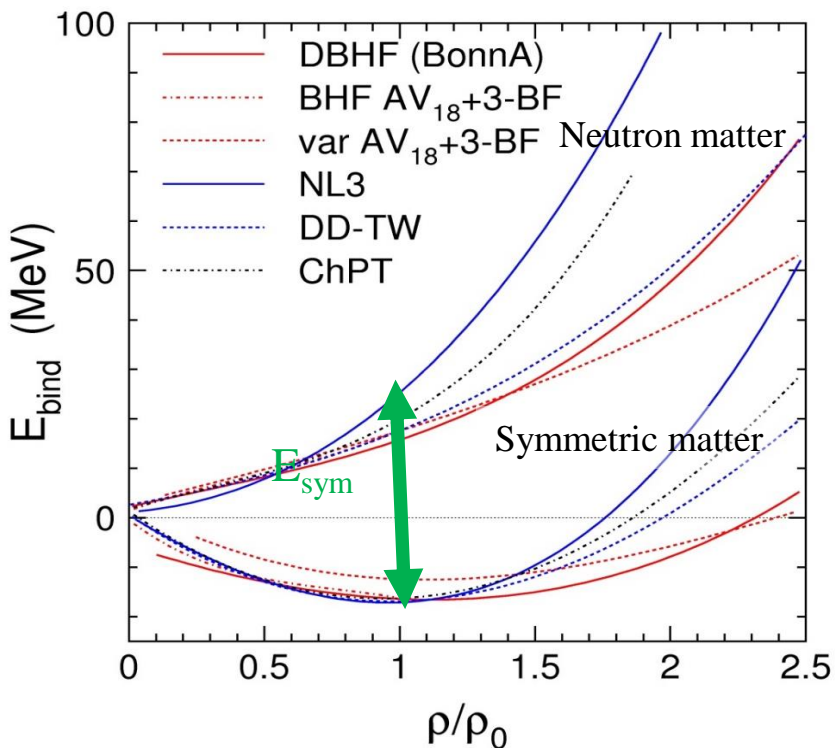
$$\frac{E}{A} = m_N + E_A(n_B) + E_{\text{sym}}(n_B) \frac{(n_p - n_n)^2}{n_B^2}$$

isospin asymmetry

$$n_B = n_p + n_n$$

Symmetric matter

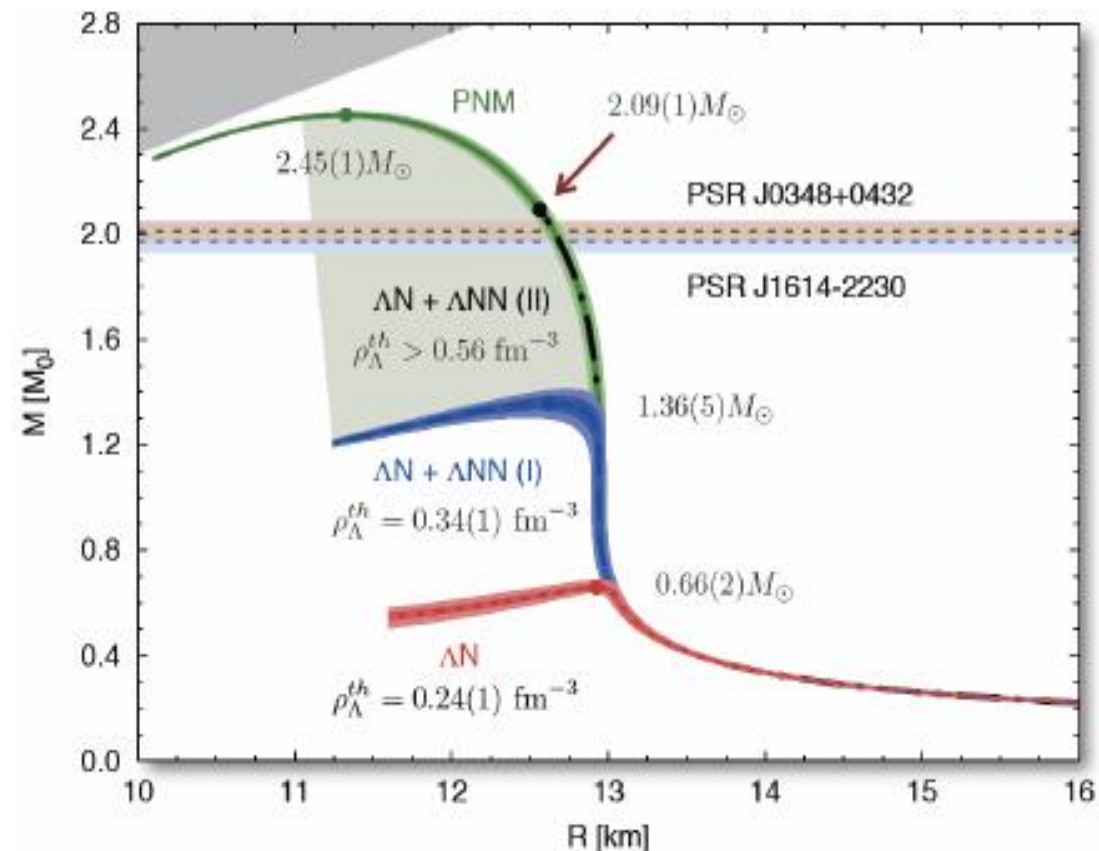
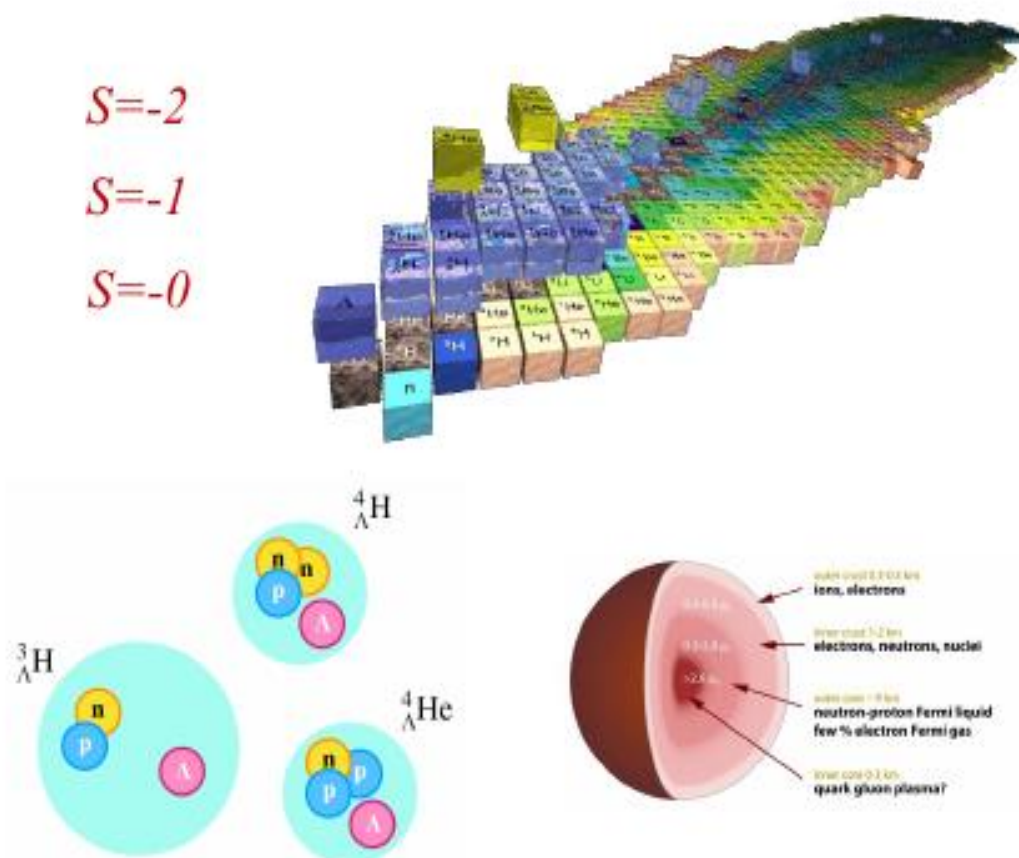
Symmetry energy



EoS describes the relation between density (n_B), pressure (P), temperature (T), energy (E), and isospin asymmetry ($(n_p - n_n)/n_B$)

Hyperon and Hyper-Nuclei Production in Heavy-Ion Collisions and Neutron Stars

PRL114, 092301(2015), HYP2018, 1512.06832, 1711.07521



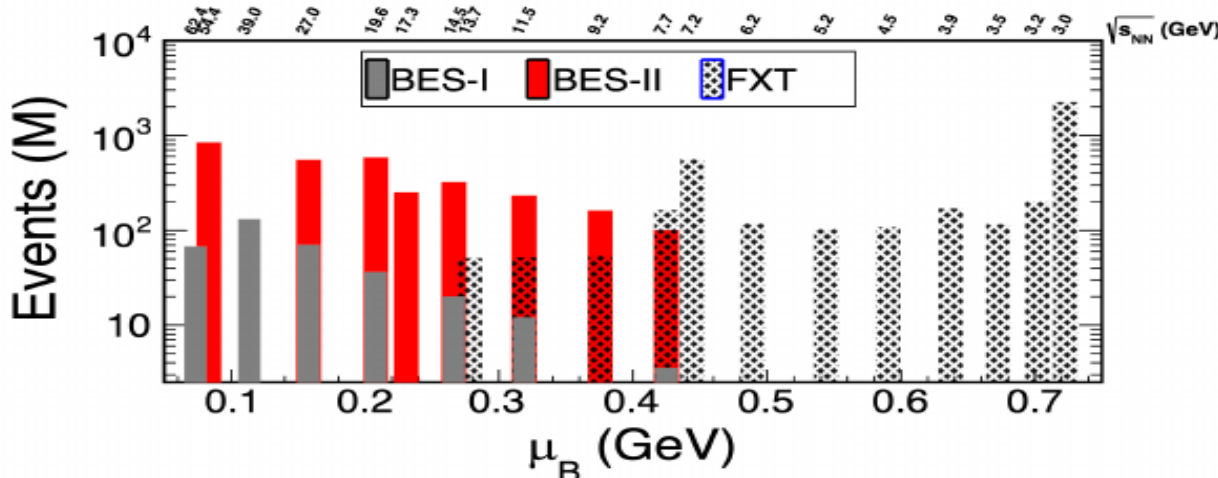
Hyperon and Hyper-Nuclei production provide access to the hyperon–nucleon interactions: NY, YNN, : key to understand the EoS at high baryon density and inner structure of neutron star.

Mass-Radius relation is “unique” to the underlying EoS

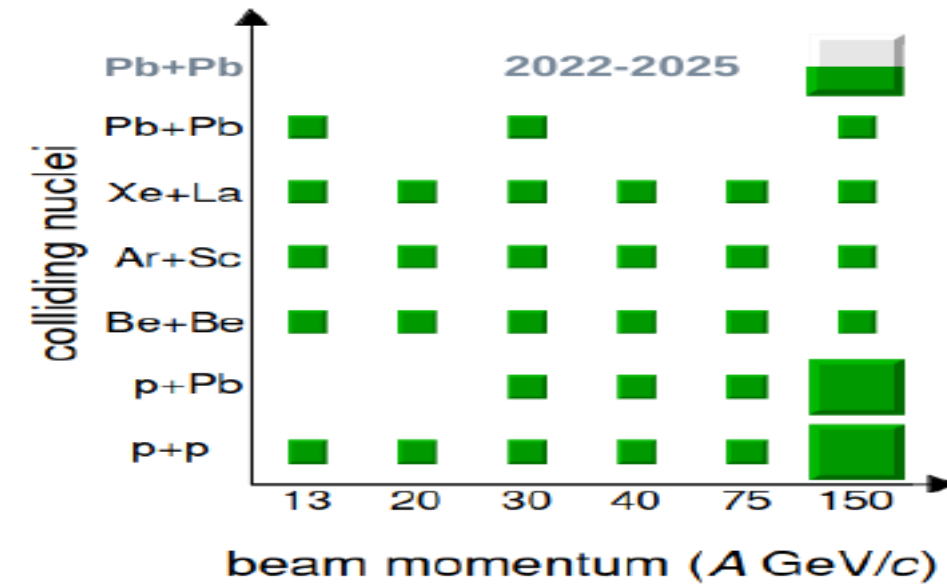
- Soft EoS: low maximum mass and small radii
- Stiff EoS: high maximum mass and large radii

Beam Energy Scan programs

STAR at RHIC: $3 < \sqrt{s_{NN}} < 200$ GeV ($750 < \mu_B < 25$ MeV)

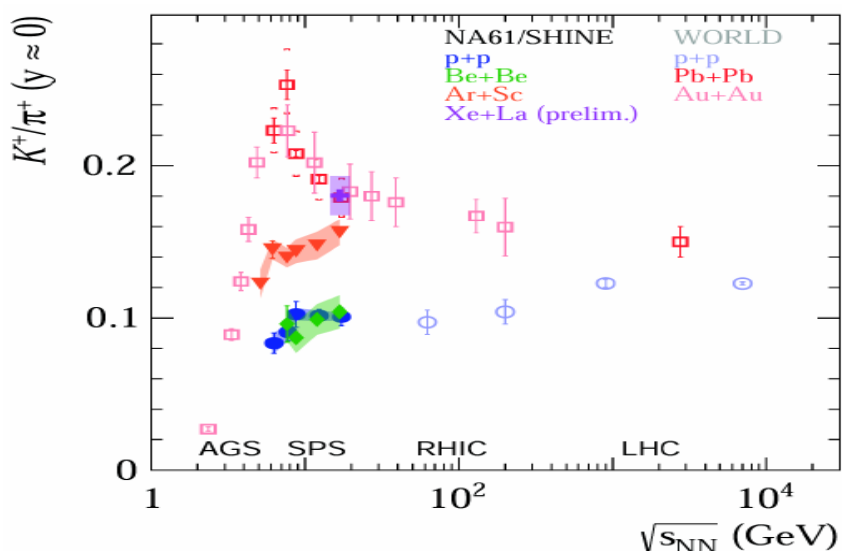


NA61SINE at SPS: $5.1 < \sqrt{s_{NN}} < 17$ (27) GeV



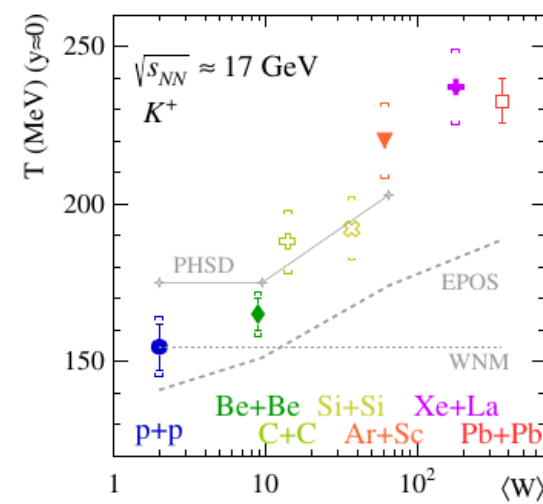
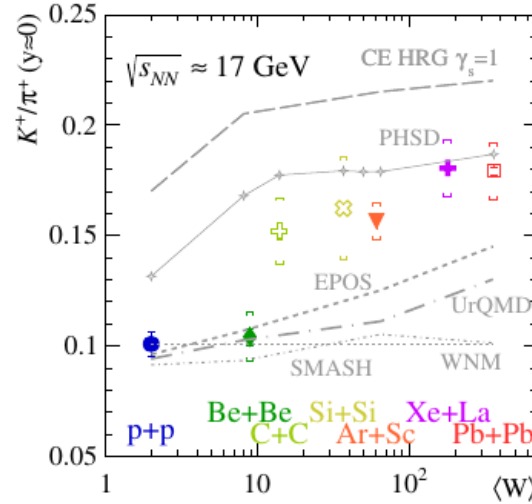
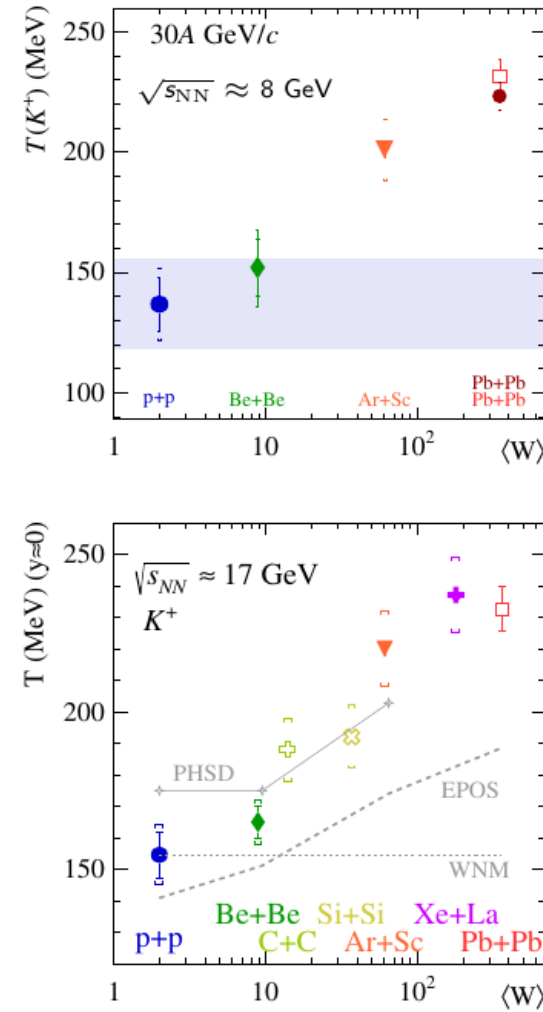
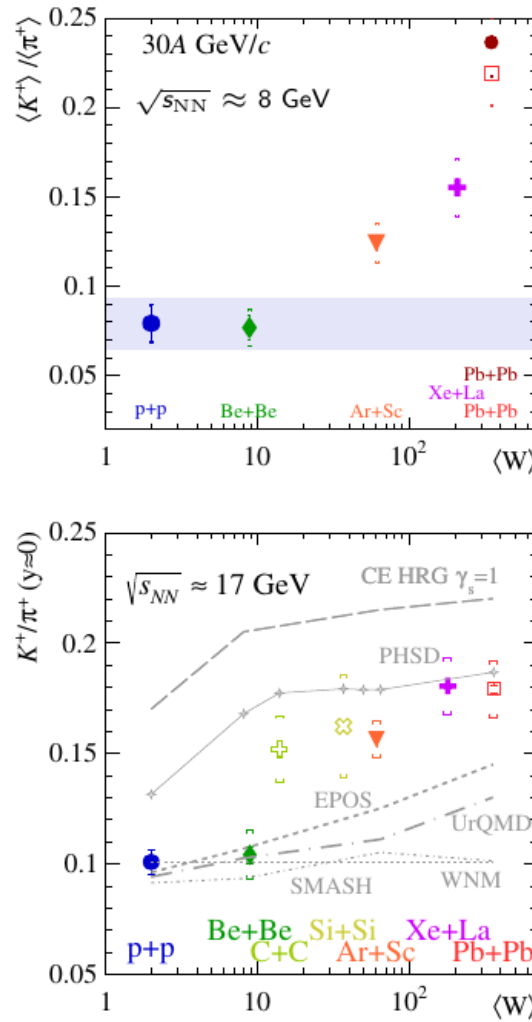
Au+Au Collisions at RHIC

Collider Runs					Fixed-Target Runs				
$\sqrt{s_{NN}}$ (GeV)	#Events	μ_B	y_{beam}	run	$\sqrt{s_{NN}}$ (GeV)	#Events	μ_B	y_{beam}	run
1 200	380 M	25 MeV	5.3	Run-10, 19	1	13.7 (100)	50 M	280 MeV	-2.69
2 62.4	46 M	75 MeV		Run-10	2 115 (70)	50 M	320 MeV	-2.51	Run-21
3 54.4	1200 M	85 MeV		Run-17	3 9.2 (44.5)	50 M	370 MeV	-2.28	Run-21
4 39	86 M	112 MeV		Run-10	4 7.7 (31.2)	260 M	420 MeV	-2.1	Run-18, 19, 20
5 27	585 M	156 MeV	3.36	Run-11, 18	5 7.2 (26.5)	470 M	440 MeV	-2.02	Run-18, 20
6 19.6	595 M	206 MeV	3.1	Run-11, 19	6 6.2 (19.5)	120 M	490 MeV	1.87	Run-20
7 17.3	256 M	230 MeV		Run-21	7 5.2 (13.5)	100 M	540 MeV	-1.68	Run-20
8 14.6	340 M	262 MeV		Run-14, 19	8 4.5 (9.8)	110 M	590 MeV	-1.52	Run-20
9 11.5	157 M	316 MeV		Run-10, 20	9 3.9 (7.3)	120 M	633 MeV	-1.37	Run-20
10 9.2	160 M	372 MeV		Run-10, 20	10 3.5 (5.75)	120 M	670 MeV	-1.2	Run-20
11 7.7	104 M	420 MeV		Run-21	11 3.2 (4.59)	200 M	699 MeV	-1.13	Run-19
					12 3.0 (3.85)	2000 M	750 MeV	-1.05	Run-18, 21



System size dependence of K/π and T

- (Rapid) changes of observables when moving from small ($p+p$, $\text{Be}+\text{Be}$) to intermediate and large ($\text{Ar}+\text{Sc}$, $\text{Xe}+\text{La}$, $\text{Pb}+\text{Pb}$) systems
- None of the models can fully reproduce the system size dependence of K^+/π^+ and T



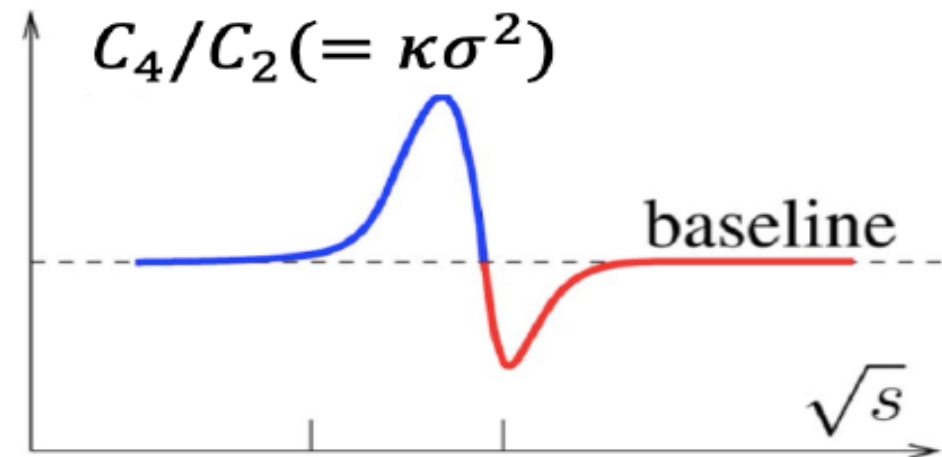
$$(p+p \approx \text{Be}+\text{Be}) \leqslant \text{Ar}+\text{Sc} \leqslant (\text{Xe}+\text{La} \approx \text{Pb}+\text{Pb})$$

N : Event-by-event multiplicity

$$\delta N = N - \langle N \rangle$$

Cumulants

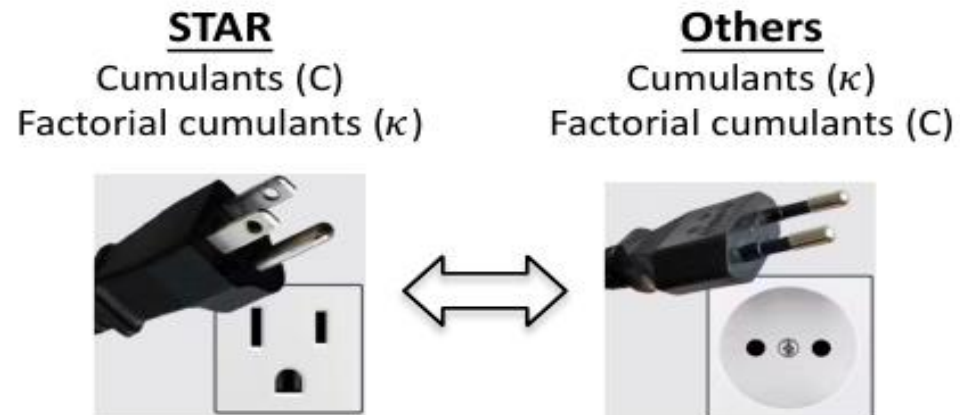
- $C_1 = \langle N \rangle$
- $C_2 = \langle \delta N^2 \rangle$
- $C_3 = \langle \delta N^3 \rangle$
- $C_4 = \langle \delta N^4 \rangle - 3\langle \delta N^2 \rangle^2$



Non-monotonic energy dependence of C_4/C_2 for the conserved baryon number (using protons as a proxy) indicates the existence of a critical region.^[1]

Factorial Cumulants

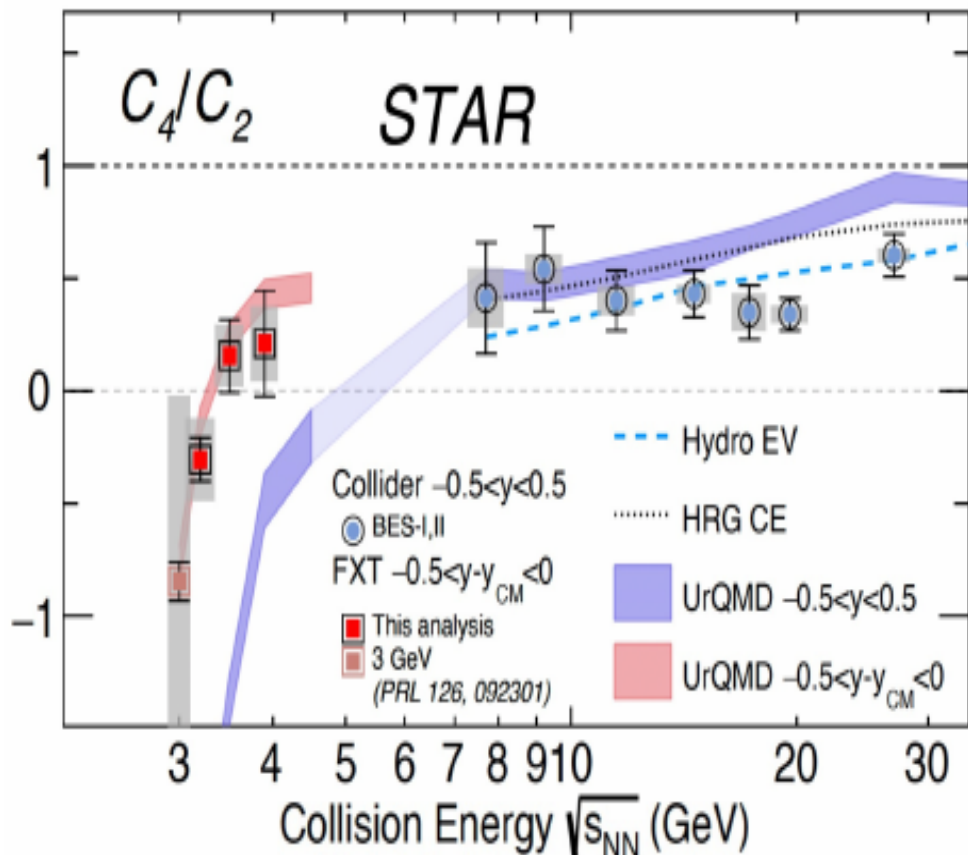
- $\kappa_1 = C_1$
- $\kappa_2 = -C_1 + C_2$
- $\kappa_3 = 2C_1 - 3C_2 + C_3$
- $\kappa_4 = -6C_1 + 11C_2 - 6C_3 + C_4$



Net-proton higher order cumulants

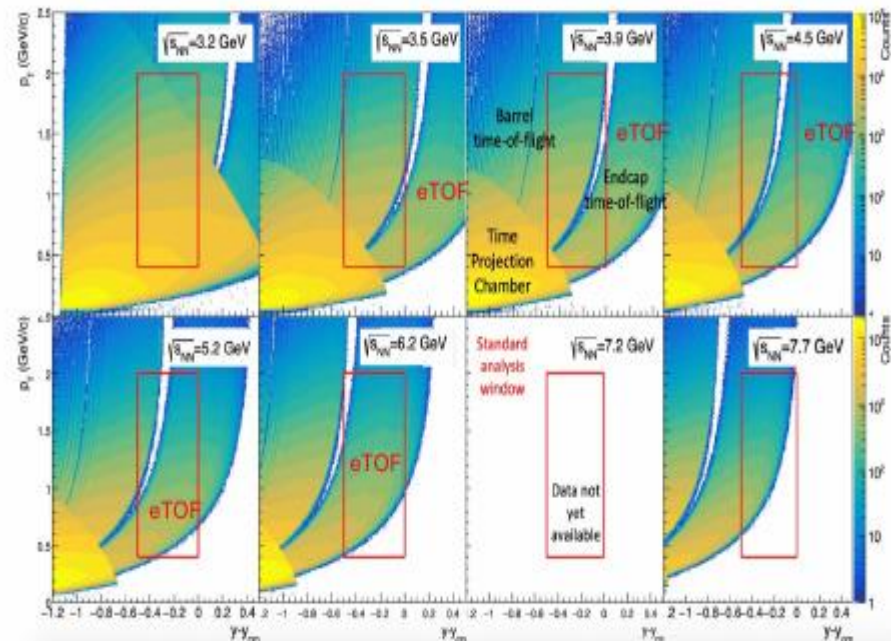
- Precision measurements from STAR BES-II
- Final results for collider energies $\sqrt{s_{NN}} = 7.7$ to 19.6 GeV and FXT energies $\sqrt{s_{NN}} = 3.2, 3.5$ and 3.9 GeV

0-5% Au+Au Collisions at RHIC



In 3.2 - 3.9 GeV, C_4/C_2 is consistent with values from UrQMD

- Deviations seen at higher energies
- Analysis of 4.5 GeV and 2 billion events from Run21 3 GeV are ongoing



Google Translate

Detect language

English German Spanish

LQCD

$$\chi_{klmn}^{BQSC} = \left. \frac{\partial^{(k+l+m+n)} [P(\hat{\mu}_B, \hat{\mu}_Q, \hat{\mu}_S, \hat{\mu}_C) / T^4]}{\partial \hat{\mu}_B^k \partial \hat{\mu}_Q^l \partial \hat{\mu}_S^m \partial \hat{\mu}_C^n} \right|_{\hat{\mu}=0}$$

Baryon number (**B**), Strangeness (**S**), Electric charge (**Q**), Cham (**C**)

0 / 5,000

EXPERIMENT Spanish

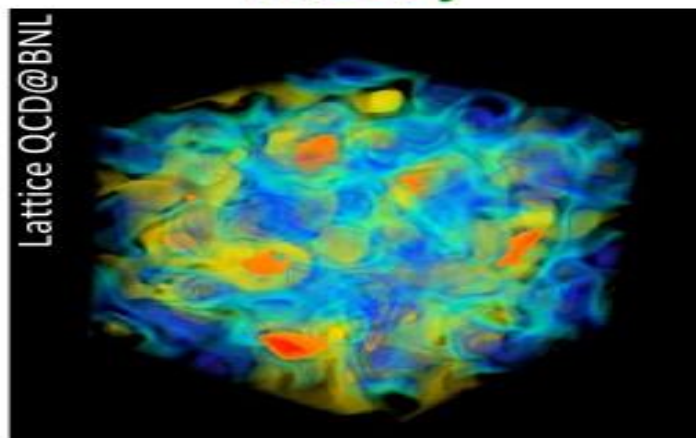
Translation

$$\chi_2^B = \frac{\kappa_2(\Delta N_B)}{V T^3} \rightarrow \frac{\kappa_4(\Delta N_B)}{\kappa_2(\Delta N_B)} = \frac{\chi_4^B}{\chi_2^B}$$

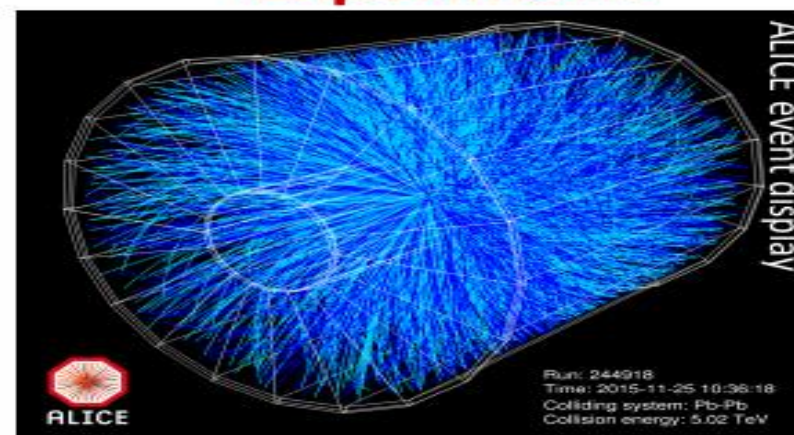
 $\kappa_n \rightarrow$ cumulants of $\Delta N_B = N_B - N_{\bar{B}}$

Bridge experimental data to LQCD calculations

Theory



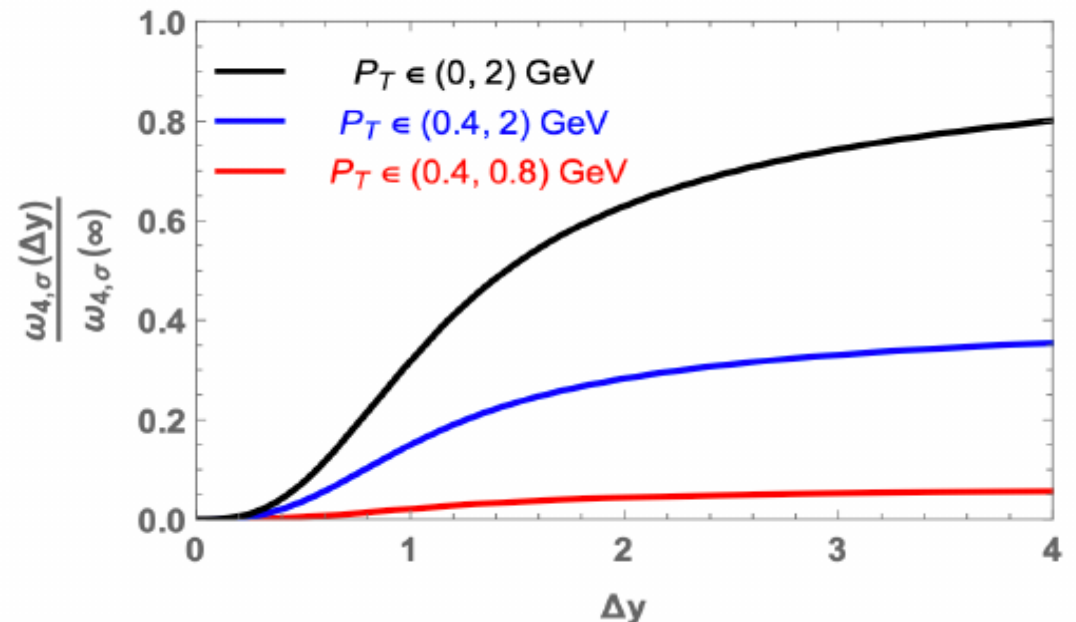
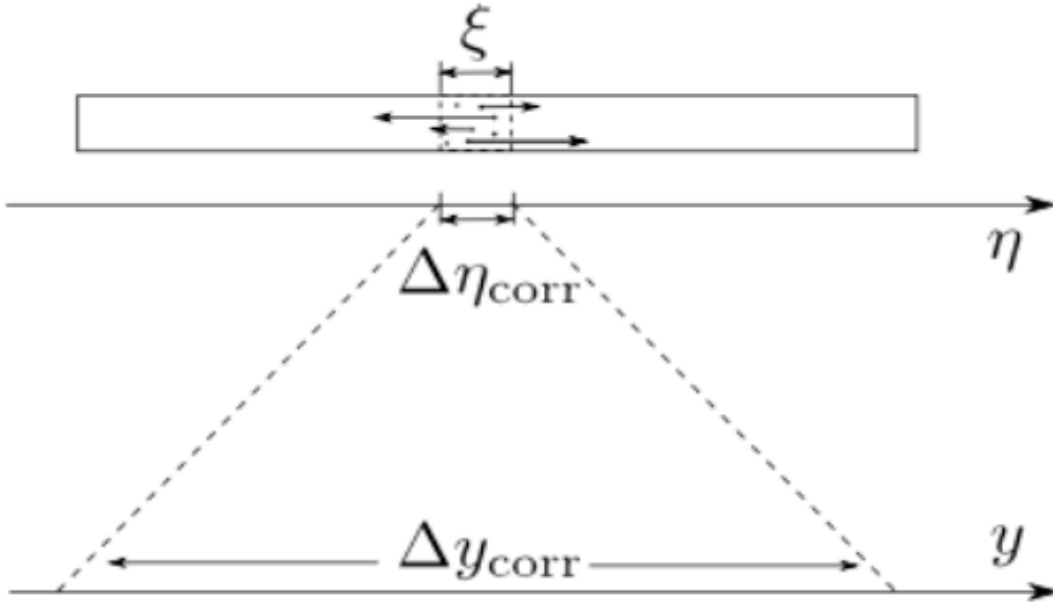
Experiment



Static
Coordinate space
Net-baryon
Fixed ∇
...

Dynamic
Momentum space
Net-proton
Fluctuating ∇
...

[1]



1. Long-range phenomena near critical point: increasing the measurement window in y and p_T magnifies the contribution to normalized cumulants;
2. For small rapidity window $\Delta y \ll \Delta y_{corr}$, and near the critical point, we expect $\kappa_n \sim (\Delta y)^n$ ^[2];
3. The wide and uniform acceptance of the detector provides us with the opportunity to conduct kinematic scan.

[1] M.A. Stephanov: Phys. Rev. Lett. 107(2011), 052301

[2] R.V. Ravai and S. Gupta: Phys. Lett. B 696(2011), 459–463

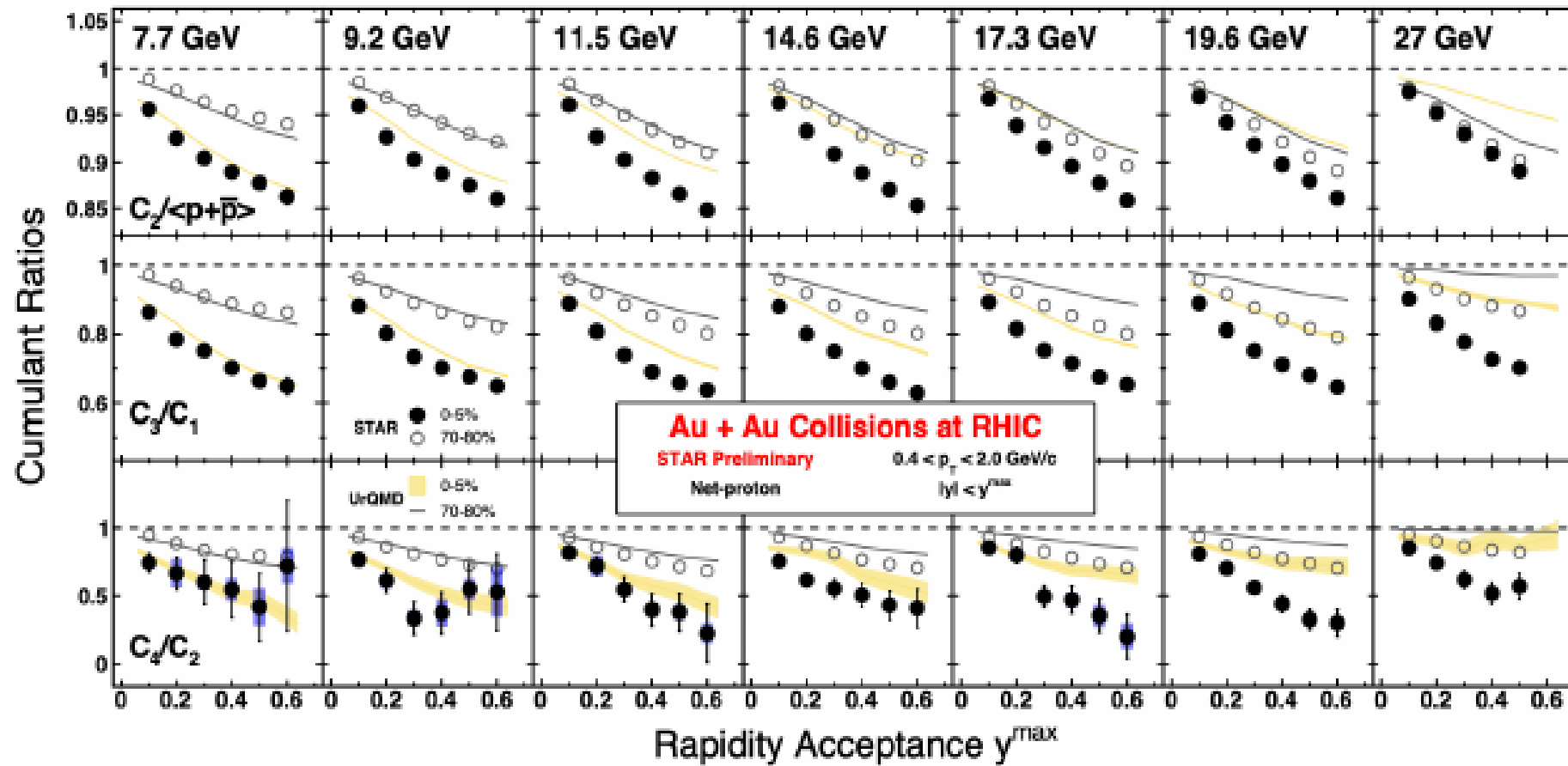
[3] S. Ejiri, F. Karsch, K. Redlich: Phys. Lett. B 633(2006), 275–282

[4] A. Bazavov, et al.: Phys. Rev. Lett. 109(2012), 192302

[5] A. Borsanyi, et al.: Phys. Rev. Lett. 111(2013), 062005

Rapidity scan of higher order cumulants

- Widening y , p_T windows of measurement enhances potential critical contributions

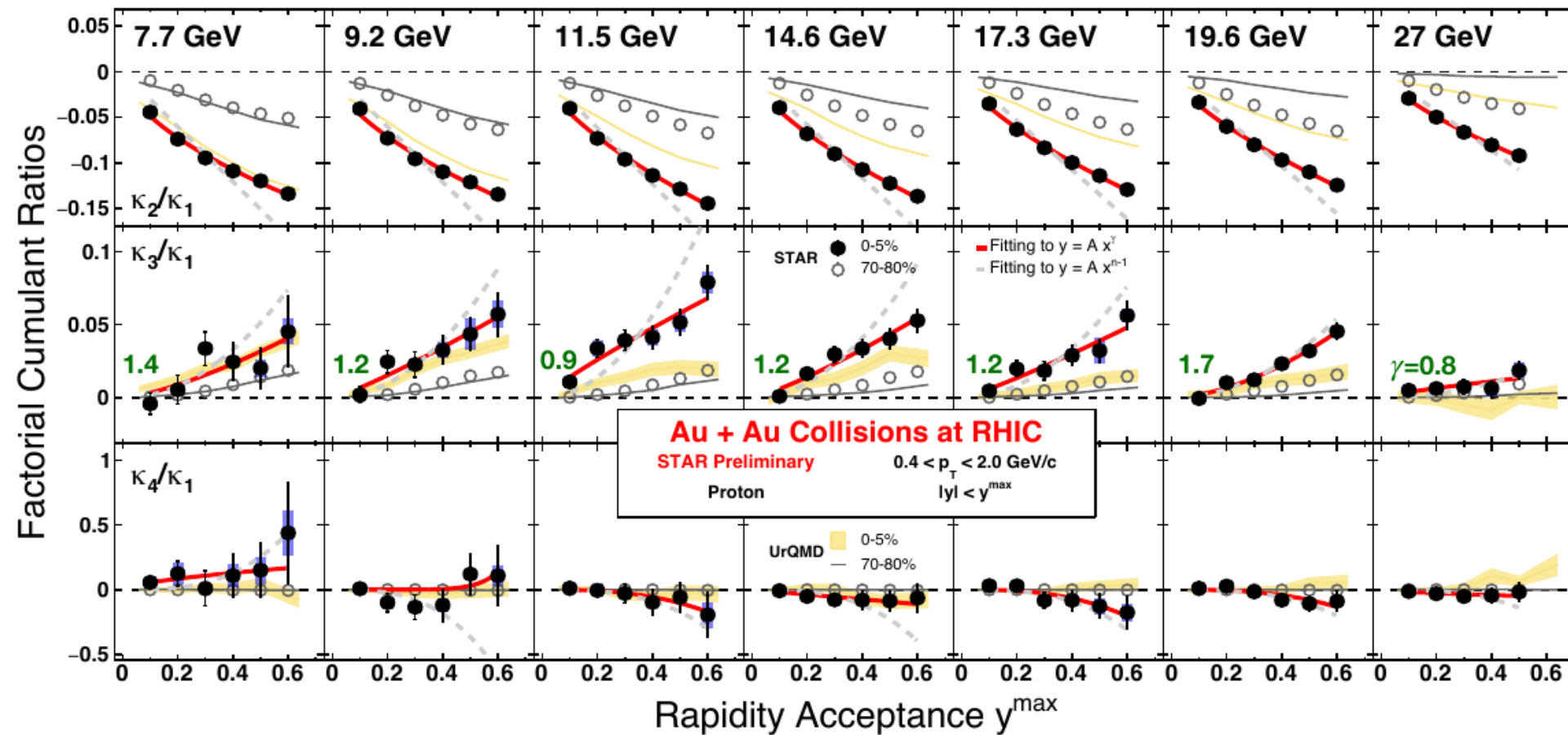


- Deviation from UrQMD increases with y acceptance and near 20 GeV

Poster by Yongcong Xu, #821

Poster by Xin Zhang #902

Proton Factorial Cumulant Ratios: Rapidity Scan



Near the critical region, factorial cumulants' dependence on Δy ($= 2 \times y^{\max}$) is simpler and are suggested to study^[1]

Deep red solid curve

(—): Fitting to $y = Ax^\gamma$

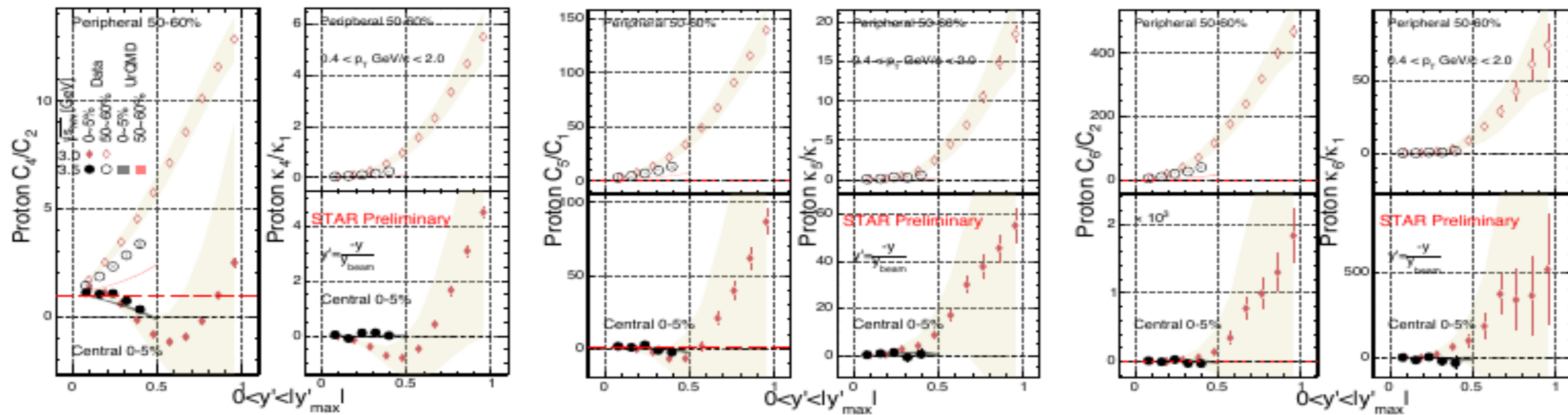
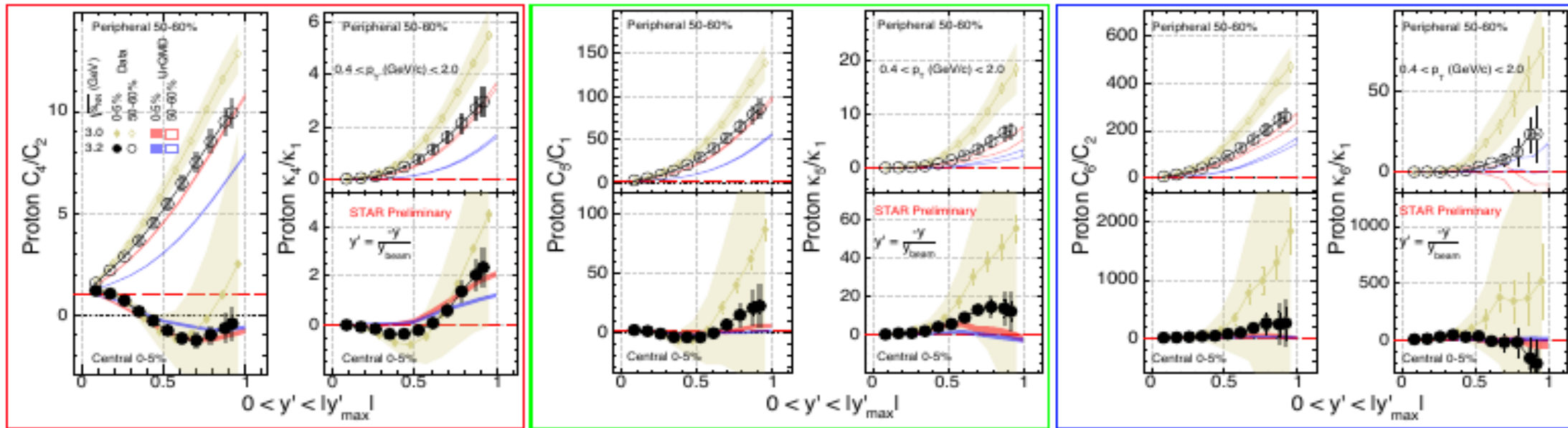
Light gray dashed curve

(---): Fitting to $y = Ax^{n-1}$

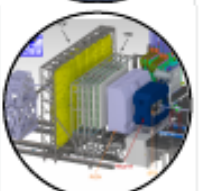
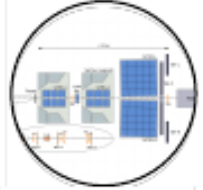
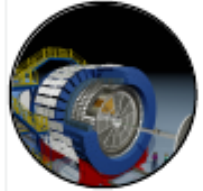
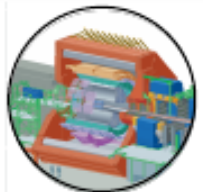
- Smaller exponents than expected power-law $\kappa_n/\kappa_1 \sim (\Delta y)^{n-1}$ are observed.

➤ Rapidity Acceptance Dependence

Y. Xu, X. Zhang, QM 2025 posters



Event-by-event fluctuations: Big picture



•
•
•

Experimental challenges:

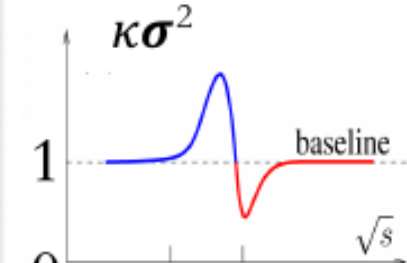
- Detection efficiency correction: Unfolding, binomial
- Event pileup: Statistical approach
- Particle identification: Fuzzy logic vs cut based particle identification
- Volume fluctuation correction (VFC): Mixed event, centrality bin width correction (CBWC)



How to interpret: “Establishing a non-critical Baseline”

- ❖ Critical fluctuations & Critical End Point (CEP) at < 5 GeV
- Global/local charge conservation
- Contribution from different hadronisation mechanisms
- Annihilation, excluded volume, resonances, hydrodynamic evolution ...

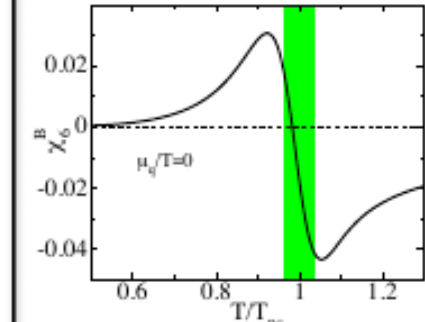
M. Stephanov,
[PRL107, 052301\(2011\)](#)



Qualitative

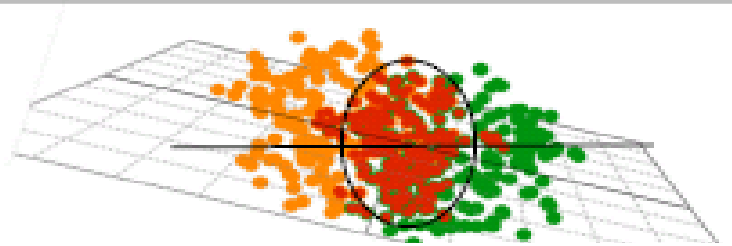


Quantitative

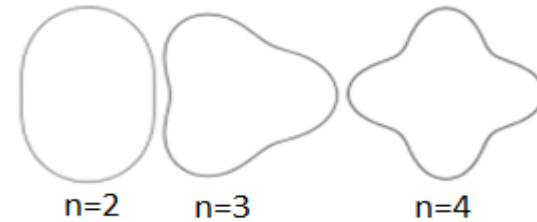


B. Friman, F. Karsch,
K. Redlich, V. Skokov
[EPJC \(2011\) 71 1694](#)

Anisotropic Flow at RHIC-LHC



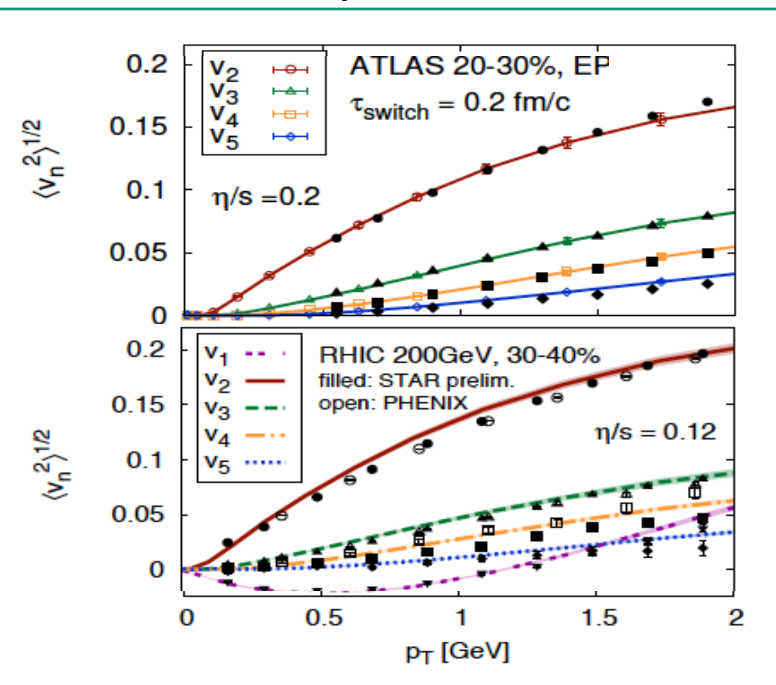
$$\epsilon_n = \sqrt{\frac{\langle r^n \cos n\phi \rangle + \langle r^n \sin n\phi \rangle}{\langle r^n \rangle}}$$



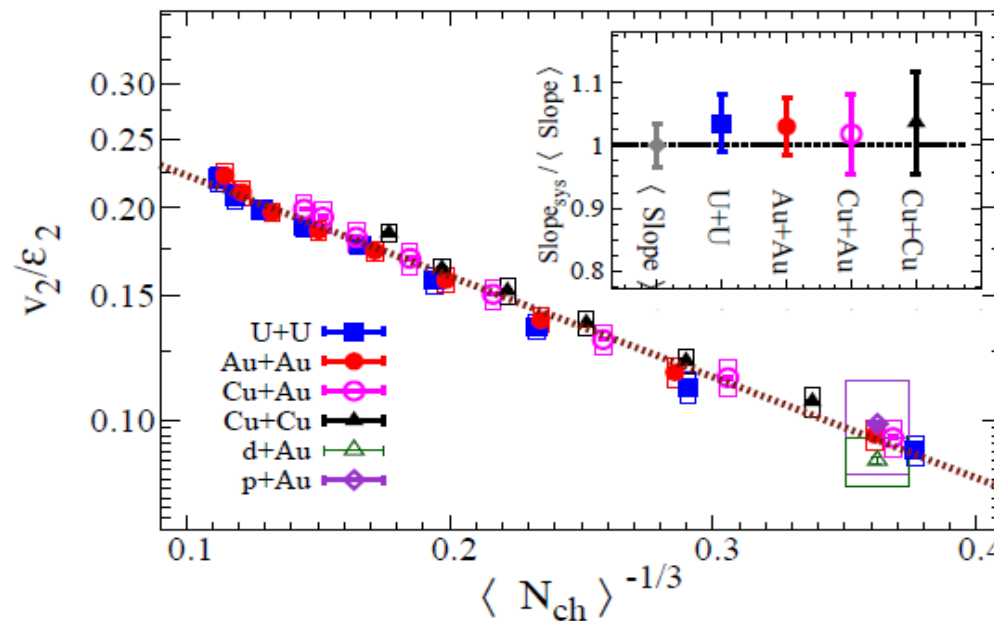
$$\frac{dN}{d\phi} \propto \left(1 + 2 \sum_{n=1} v_n \cos[n(\phi - \Psi_n)] \right)$$

Initial eccentricity (and its attendant fluctuations) ϵ_n drive momentum anisotropy v_n with specific viscous modulation

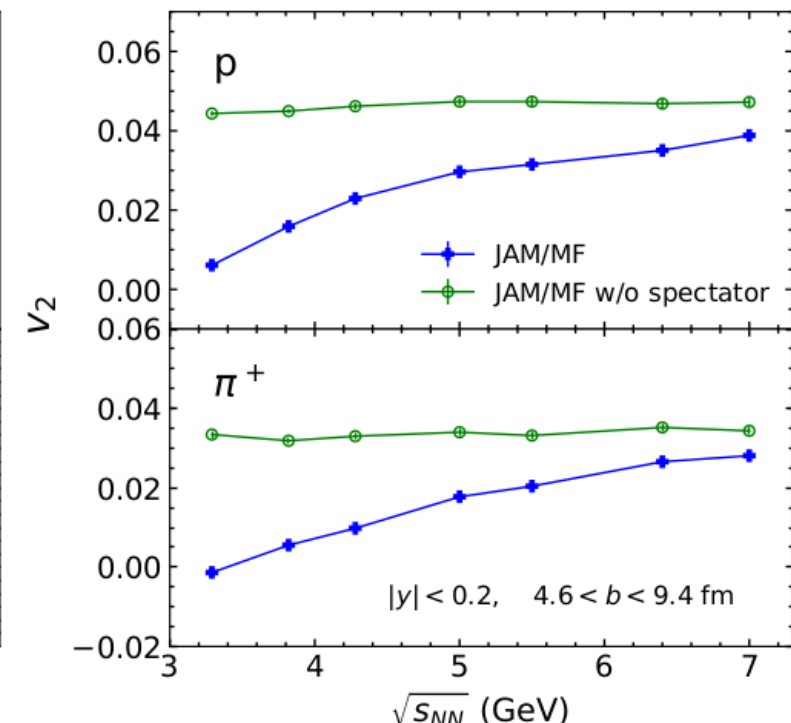
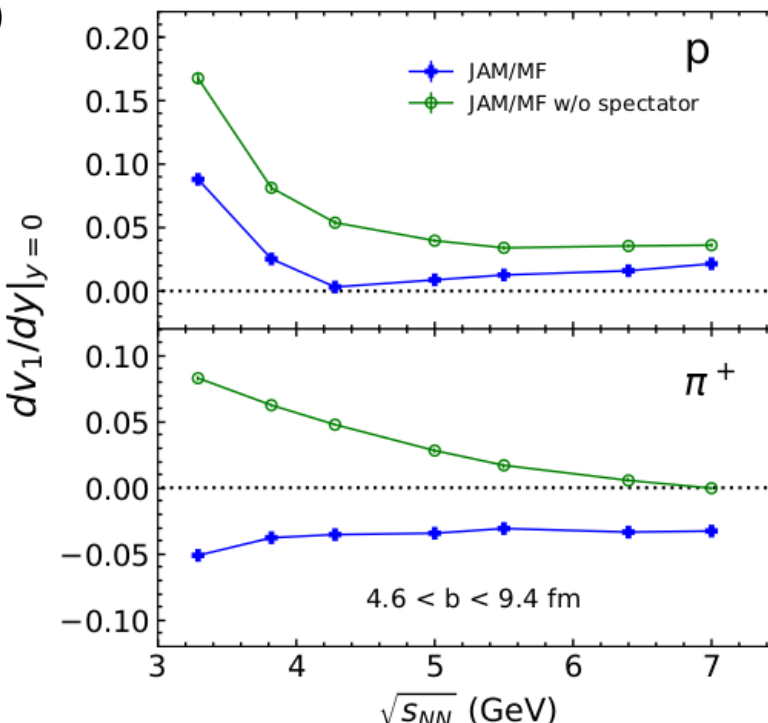
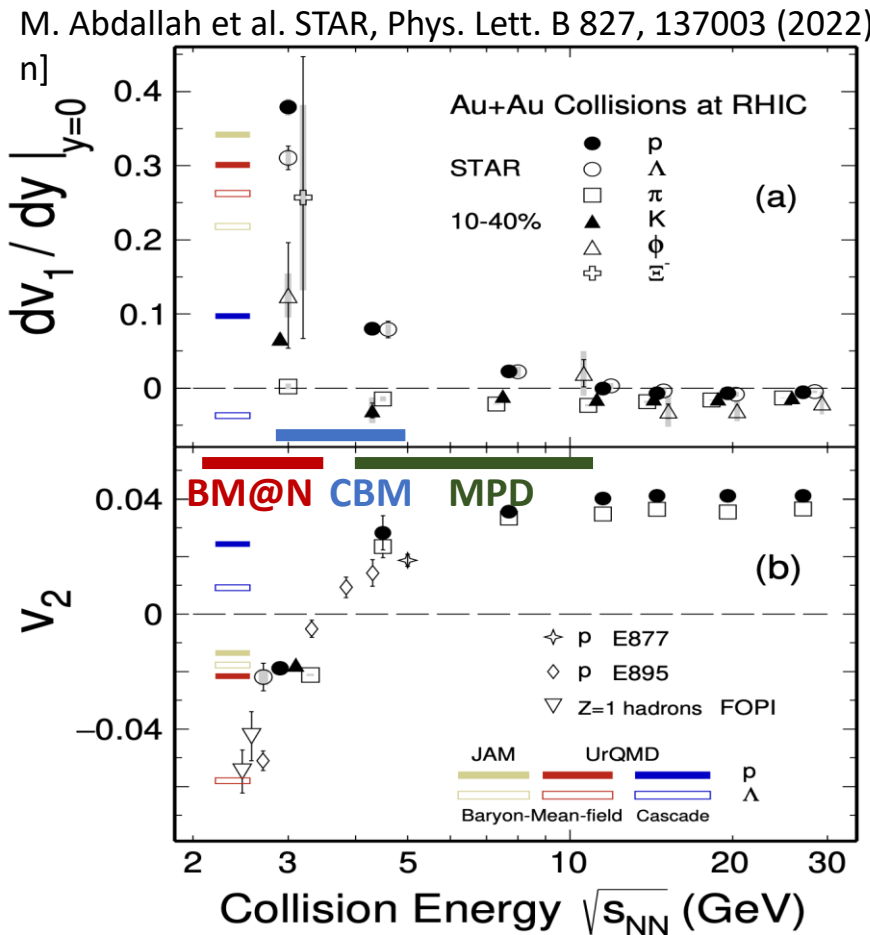
Gale, Jeon, et al., Phys. Rev. Lett. 110, 012302



STAR, Phys. Rev. Lett. 122 (2019) 172301



Anisotropic flow in heavy-ion collisions at high baryon density



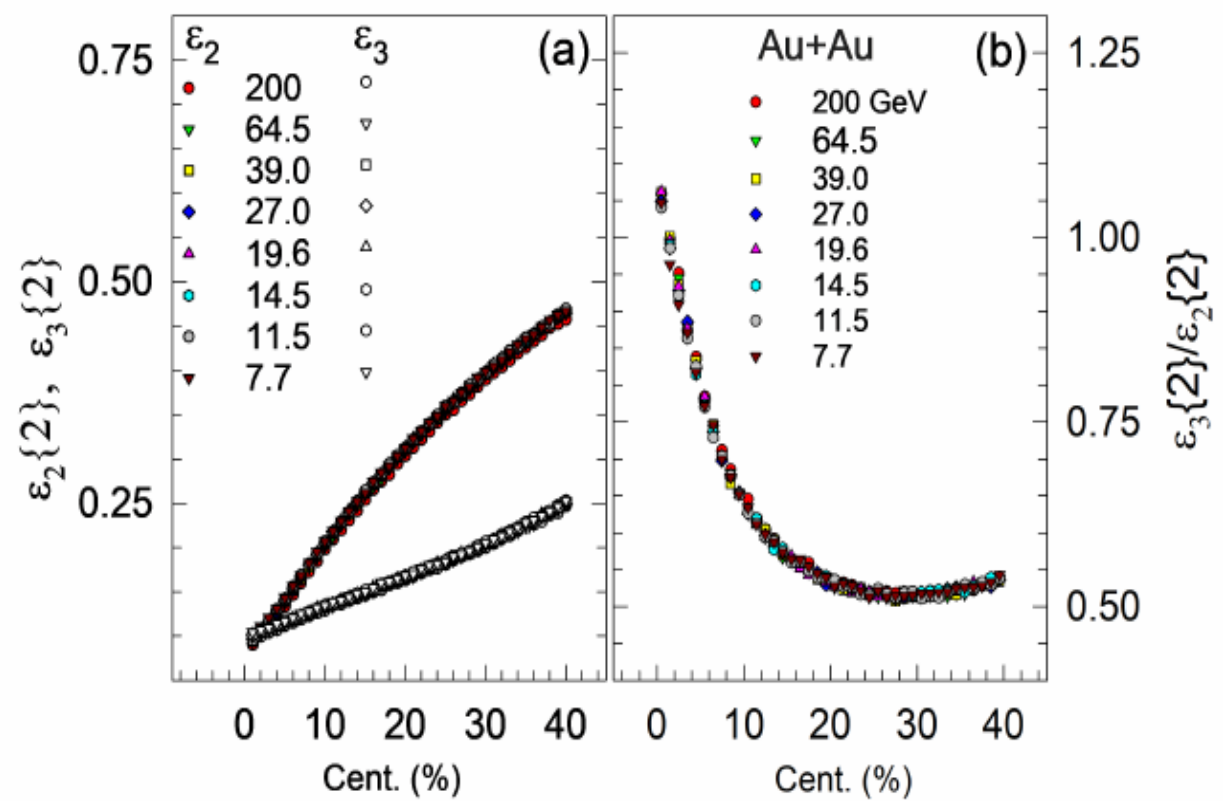
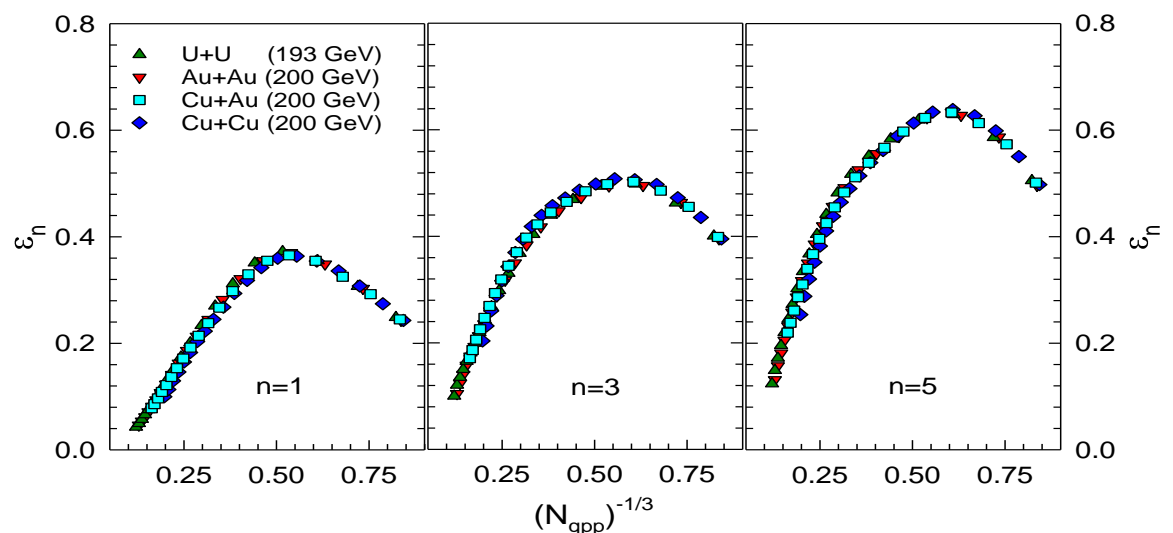
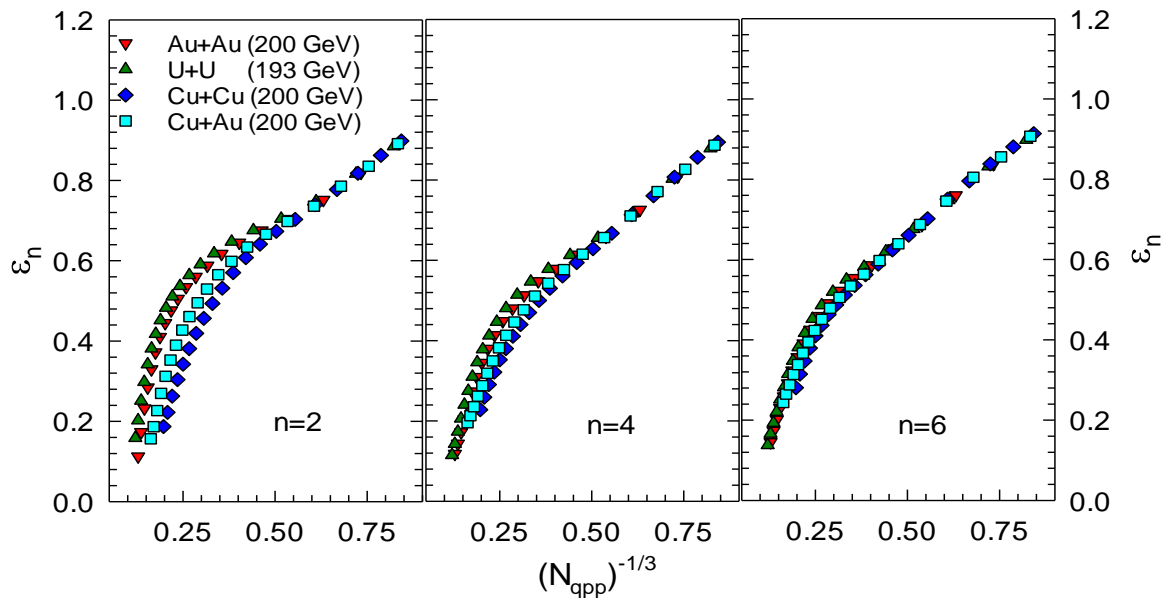
Phys. Rev. C 97, 064913 (2018)

Anisotropic flow at FAIR/NICA energies is a delicate balance between:

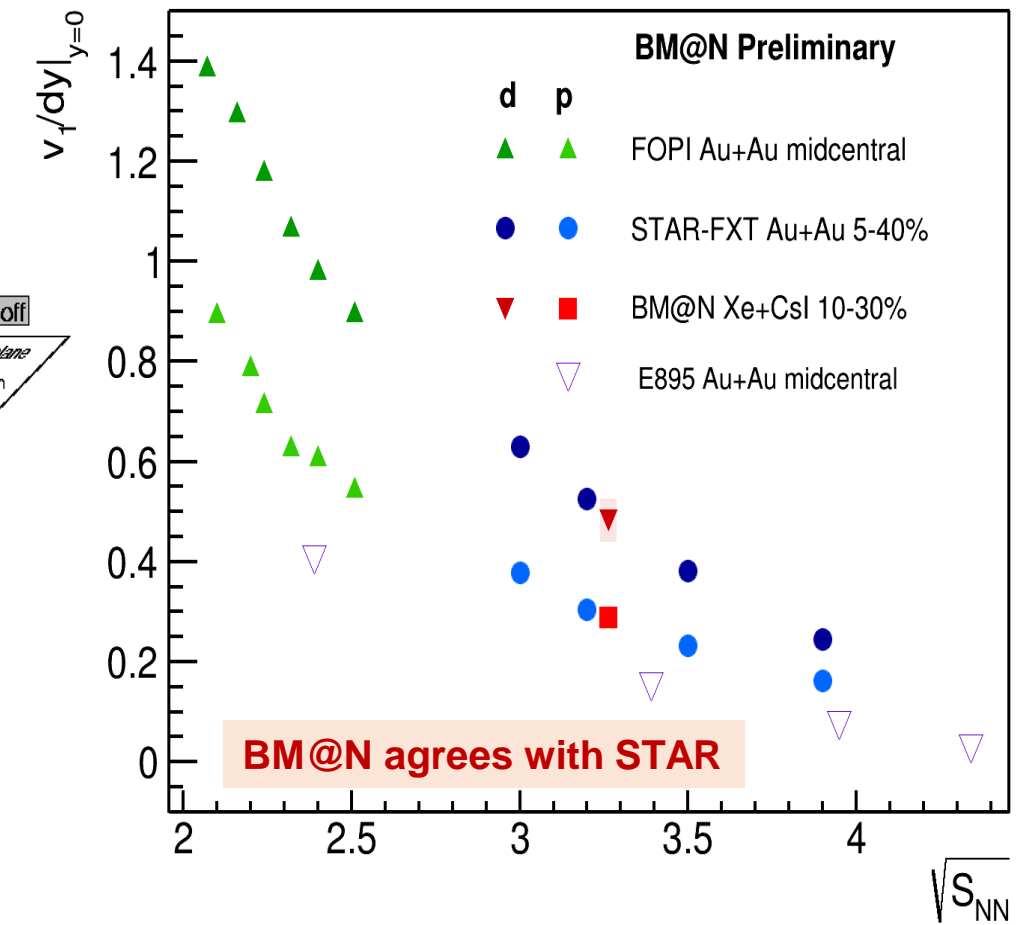
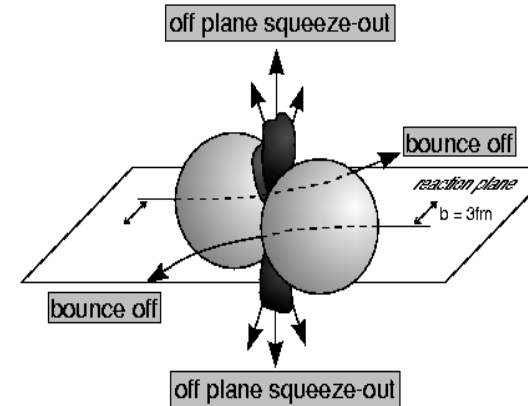
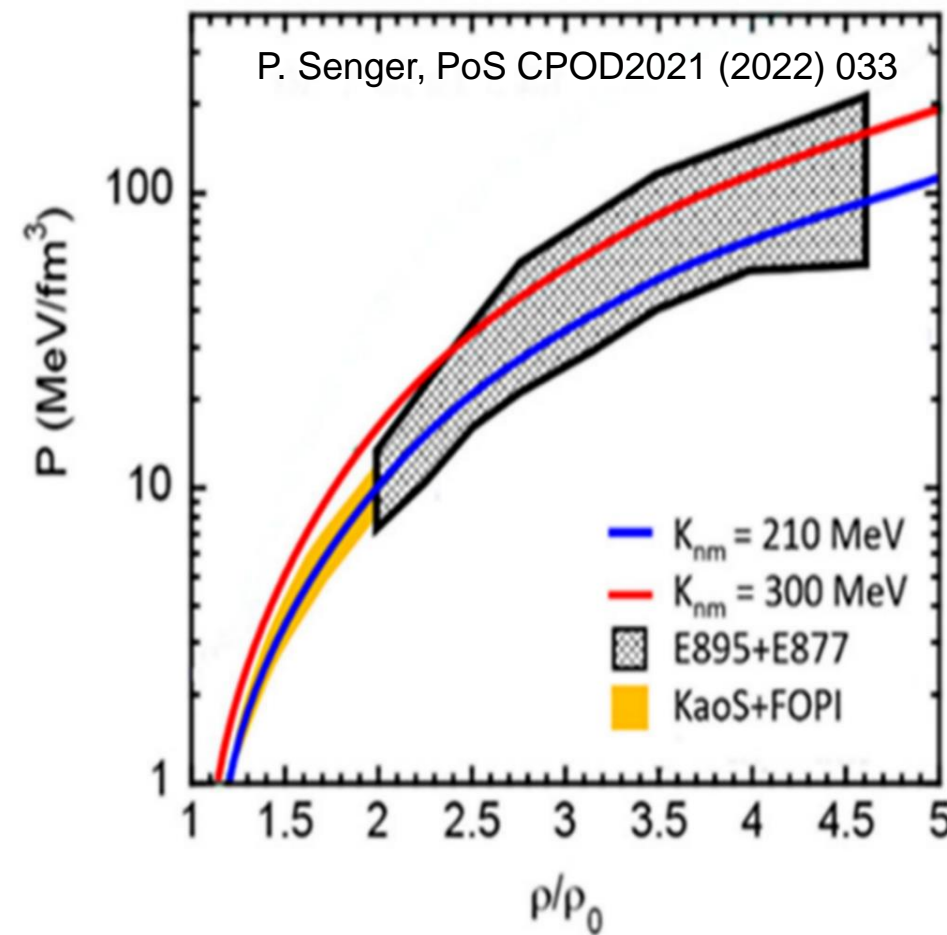
- The ability of pressure developed early in the reaction zone ($t_{exp} = R/c_s$, $c_s = c\sqrt{dp/d\varepsilon}$) and
- The passage time for removal of the shadowing by spectators ($t_{pass} = 2R/\gamma_{CM}\beta_{CM}$)

Anisotropic Flow – Expected Shapes

courtesy of R.A. Lacey



Directed flow of protons and EOS of symmetric matter

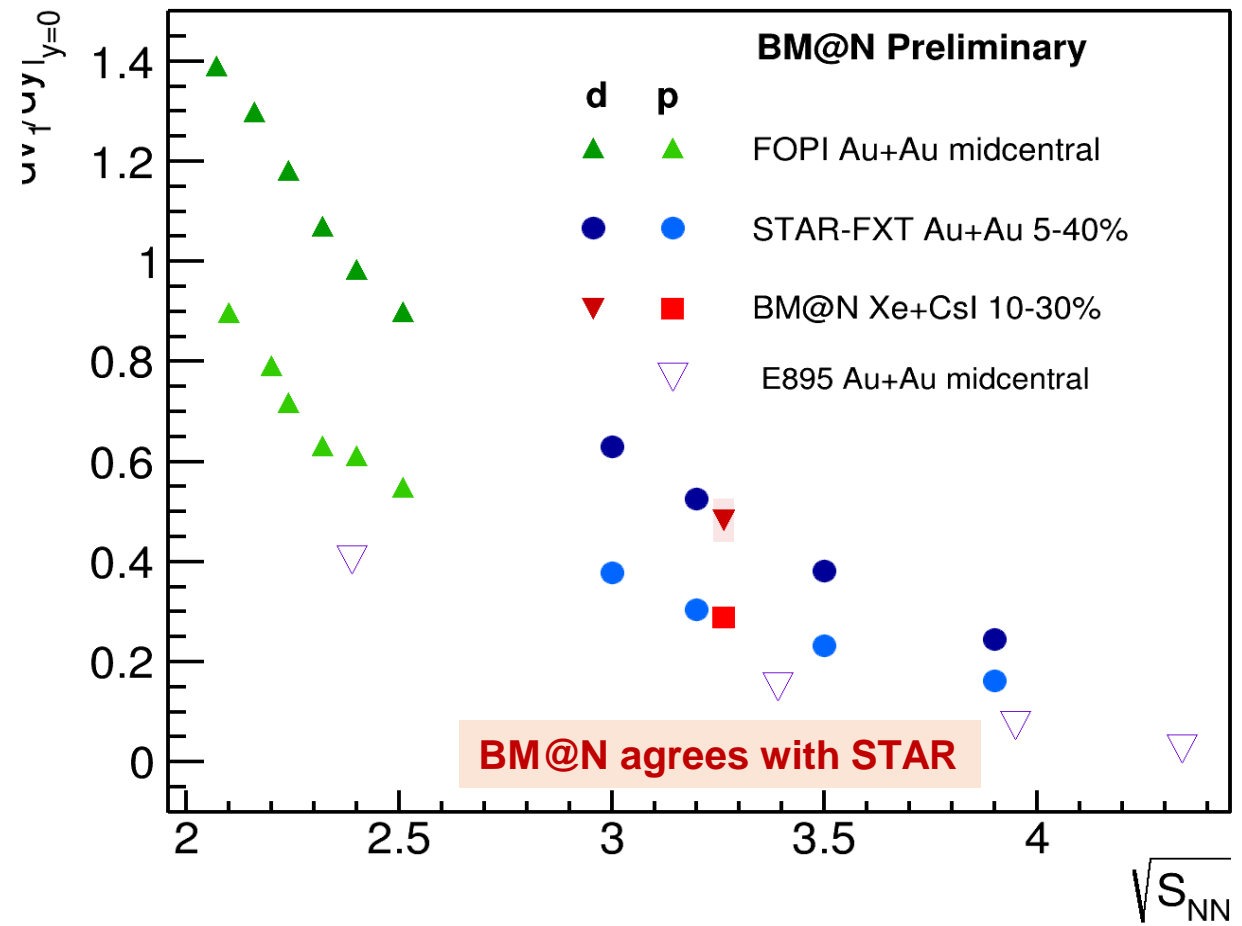
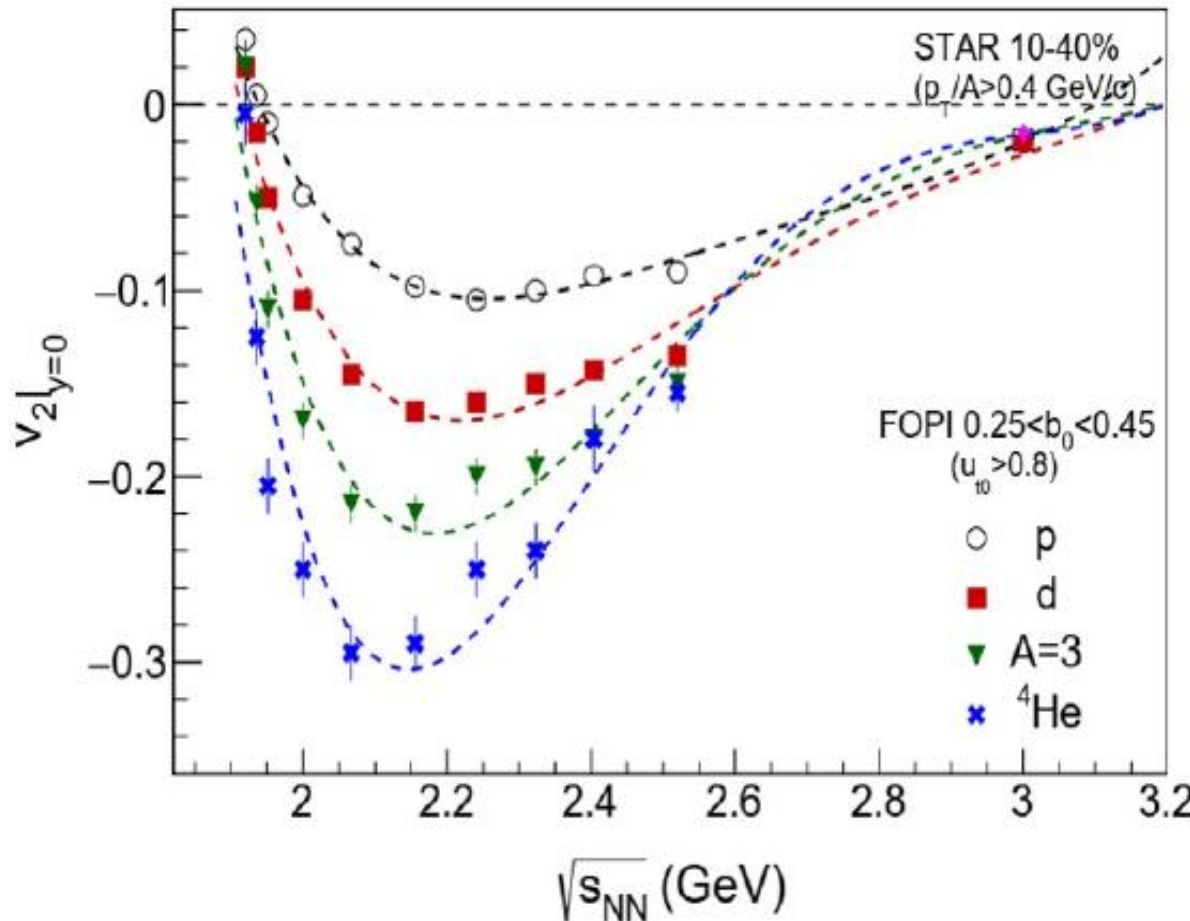


Nuclear incompressibility from collective proton flow

P. Danielewicz, R. Lacey, W.G. Lynch, Science 298 (2002) 1592

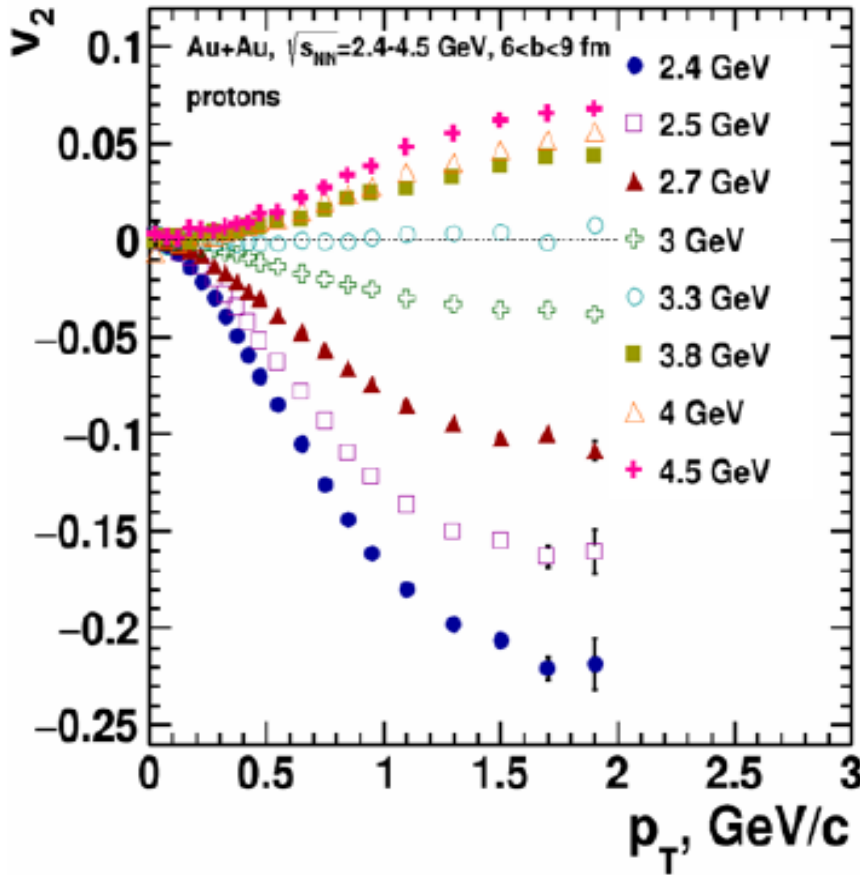
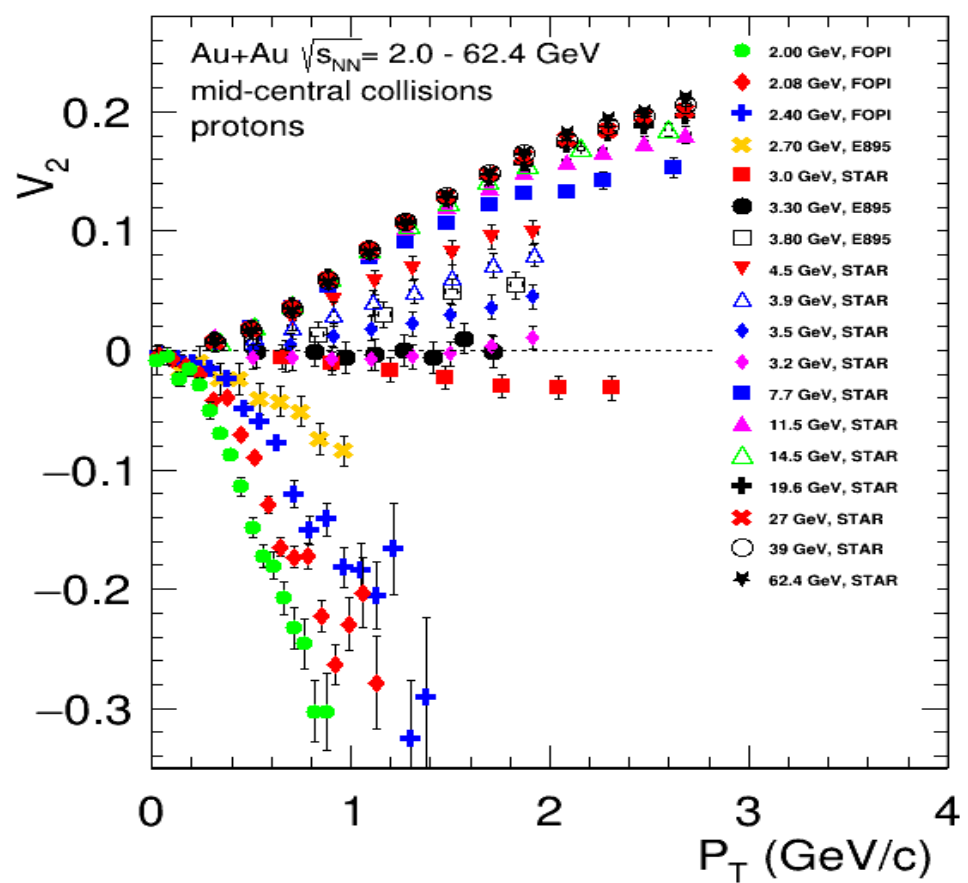
Both STAR and BM@N results for directed flow prefer stiff EOS

Directed and elliptic flows of and EOS of symmetric matter



Anisotropic flow in Au+Au collisions at Nuclotron-NICA energies

Particles 6 (2023) 2, 622-637

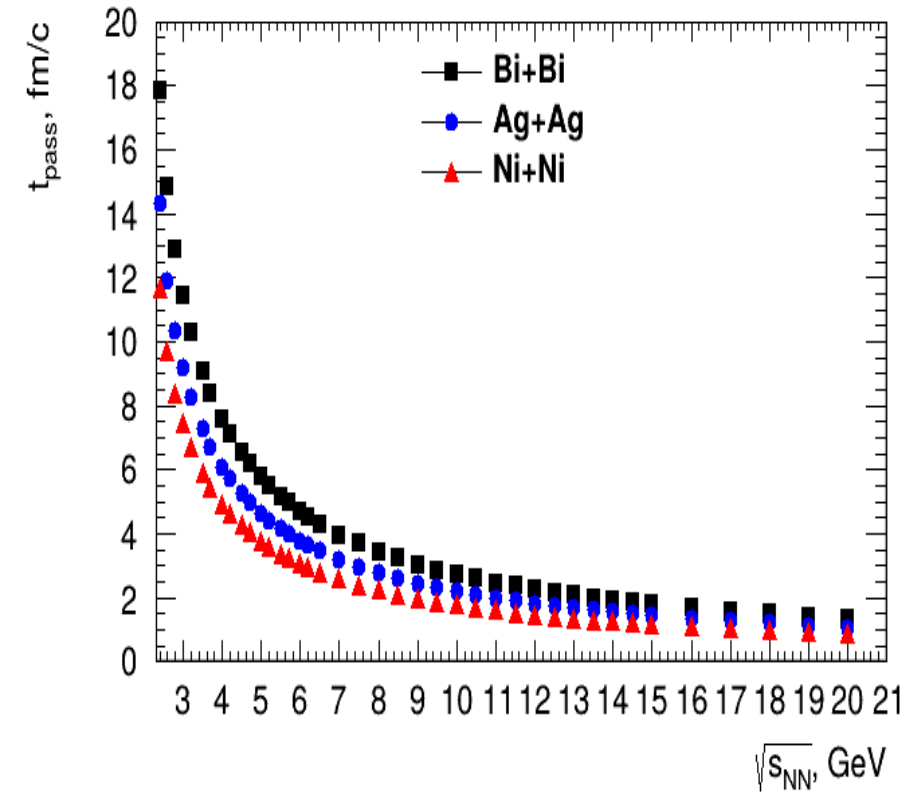
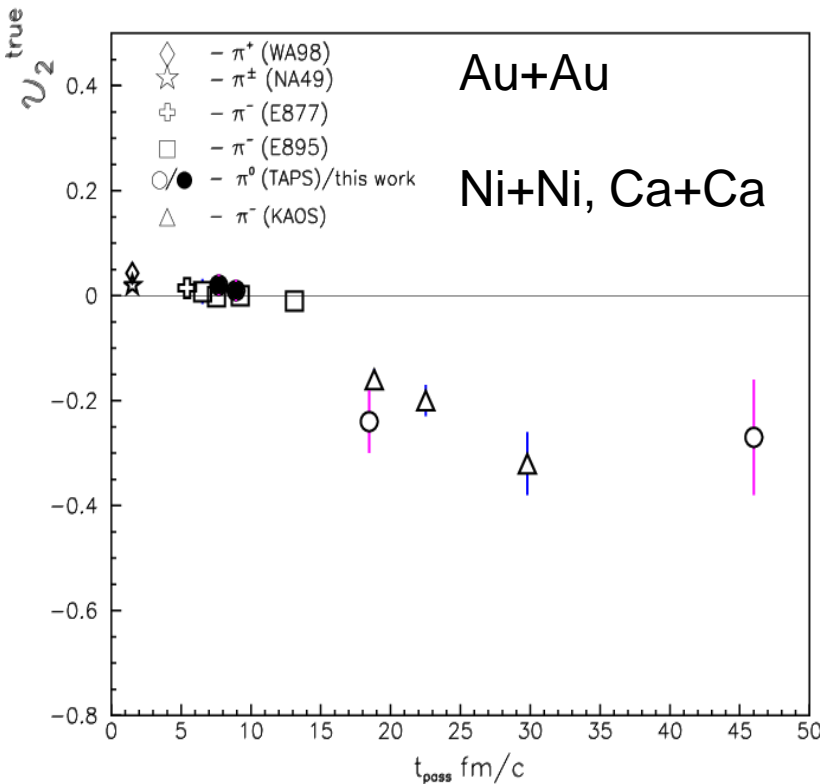
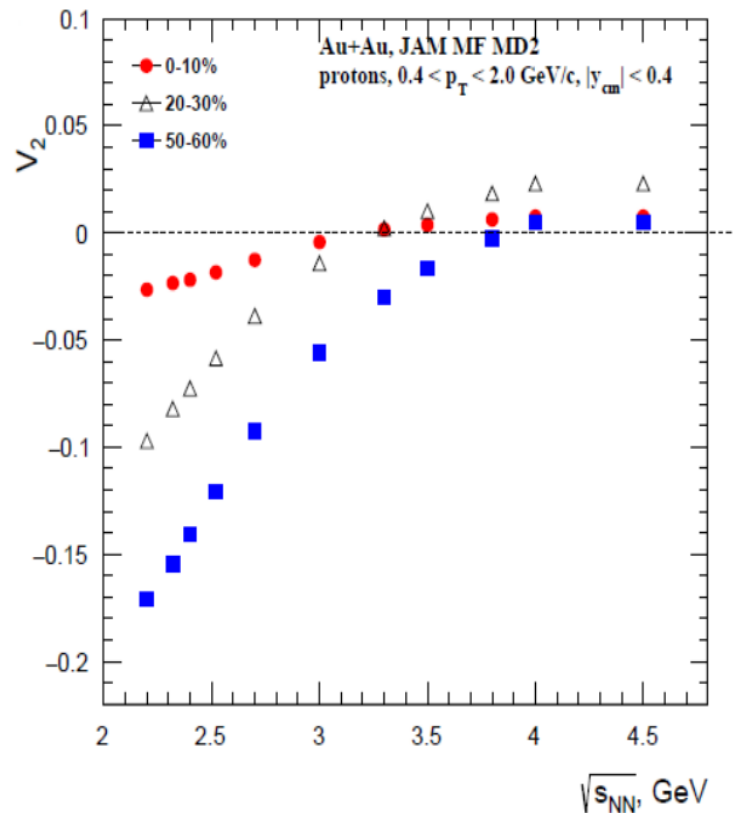


Anisotropic flow at FAIR/NICA energies is a delicate balance between:

- I. The ability of pressure developed early in the reaction zone ($t_{exp} = R/c_s$, $c_s = c\sqrt{dp/d\varepsilon}$) and
- II. The passage time for removal of the shadowing by spectators ($t_{pass} = 2R/\gamma_{CM}\beta_{CM}$)

Elliptic flow: transition from out-of-plane to in-plane: geometry

P. Parfenov, Particles 5 (2022) 4, 561-579 A.T Czech.J.Phys. 50S4 (2000) 139-166

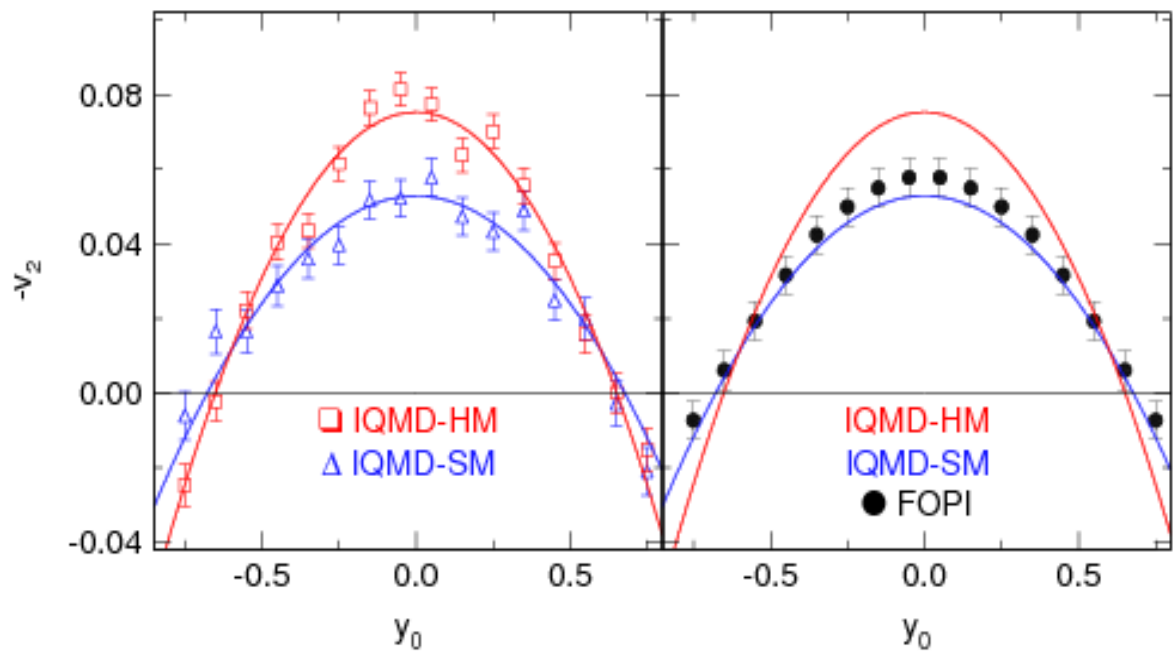


Rapidity dependence of v_2 and EOS

HM – stiff momentum dependent with $K=376$ MeV

SM – soft momentum dependent with $K=200$ MeV

Au+Au 1.2A GeV $0.25 < b_0 < 0.45$ protons



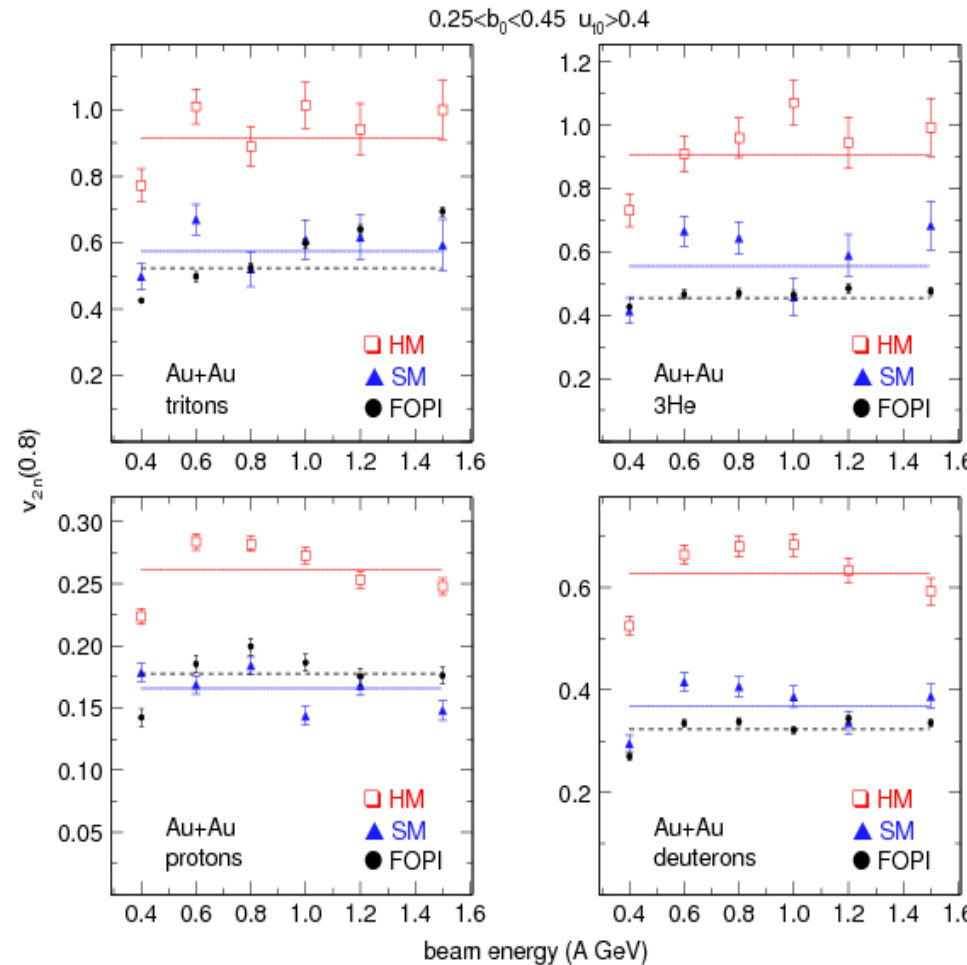
$$V2n = |V20| + |V22|$$

$$\text{Fit: } V2(y0) = V20 + V22 * Y0^2$$

Large rapidity coverage is important for flow measurements: MPD forward upgrade

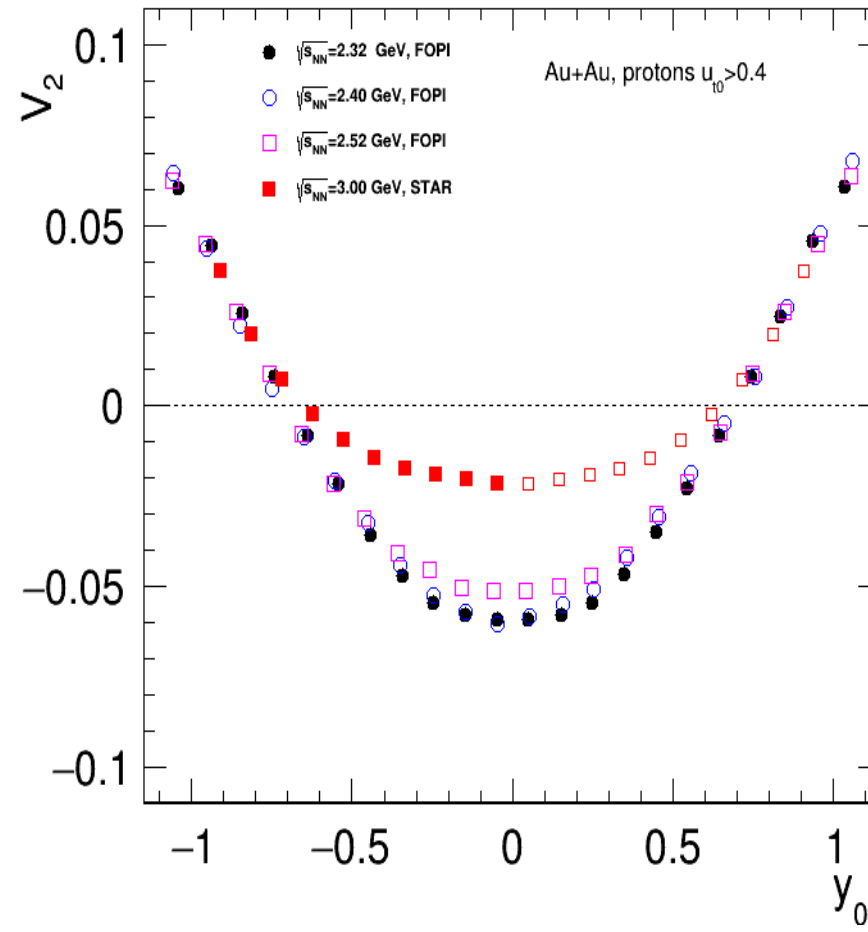
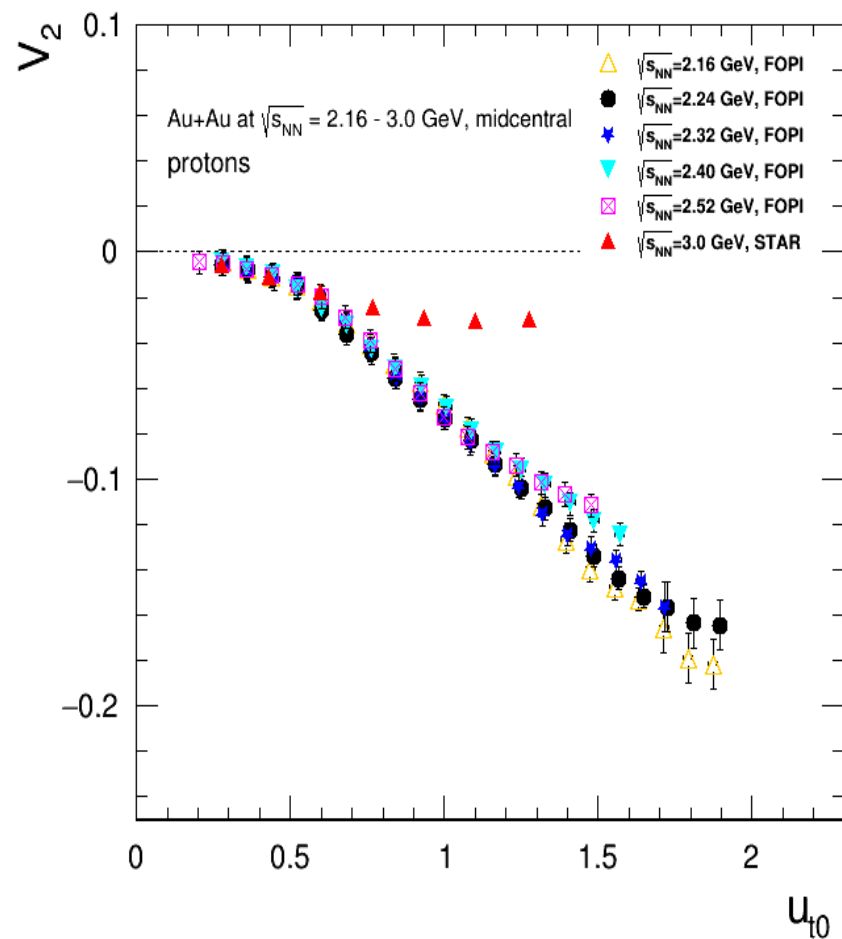
FOPI data : Nucl. Phys. A 876 (2012) 1

IQMD : Nucl Phys. A 945 (2016)



u_{t0} scaling: FOPI/STAR data

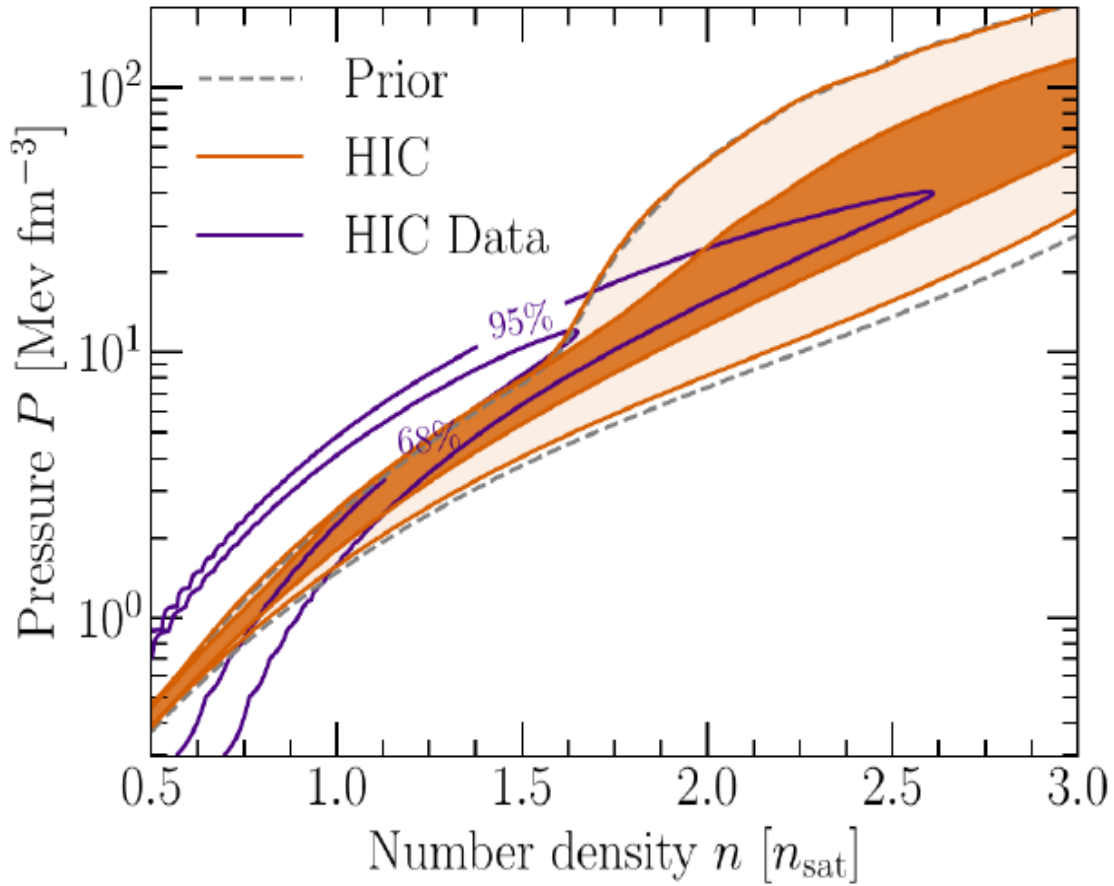
STAR published results for protons : Scaling breaks at $\sqrt{s_{NN}}=3\text{GeV}$ – but holds at forward rapidity?



Constraining neutron-star matter with microscopic and macroscopic collisions

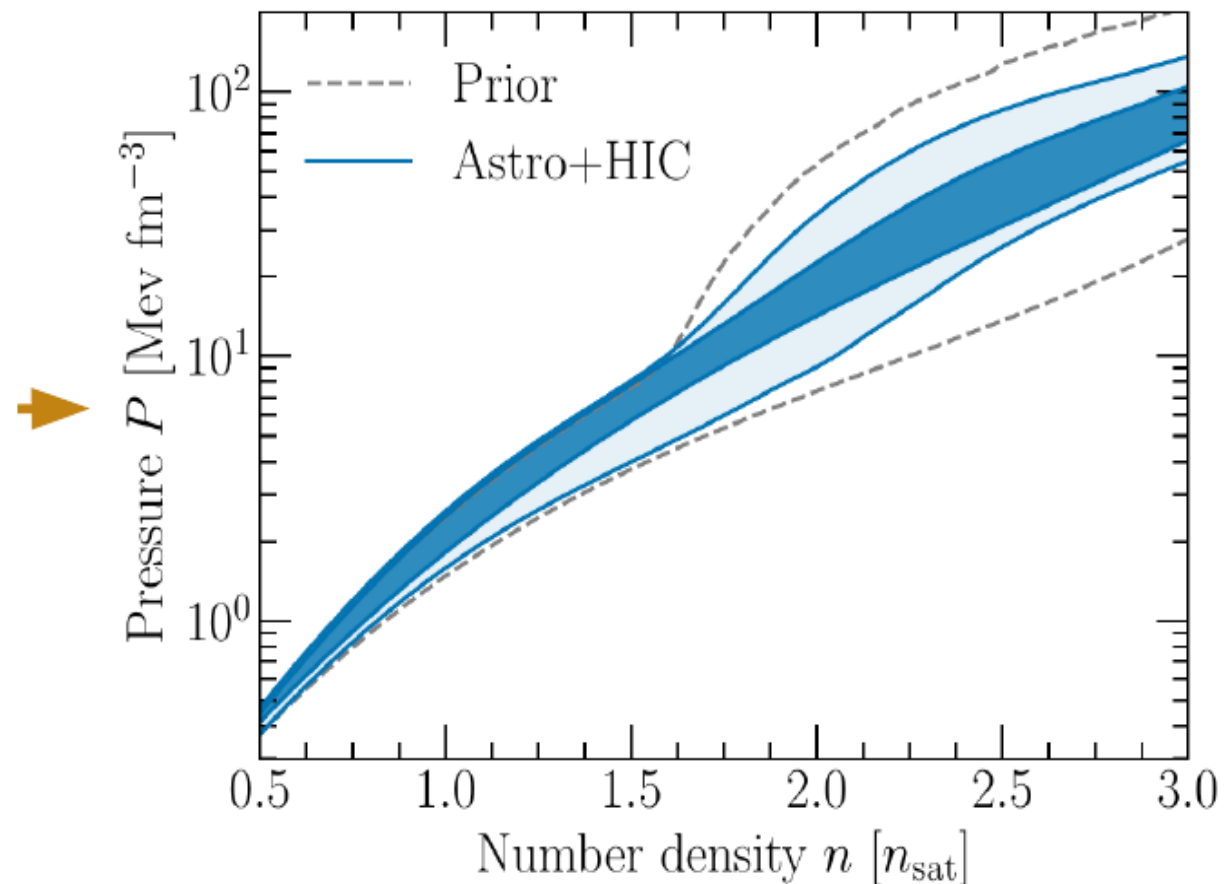
Huth, Pang et al. *Nature* 606(22)276

HIC experiments:



Bayesian combinations

HIC and Astro combined:



Astrophysical observations narrow constraints above $2 n_{\text{sat}}$

Rapidity Scan with MPD at NICA

Rapidity dependence of cumulant observables can enhance the prospect of discovering a CEP

J.Li, L.Du and S.Shi,

"Rapidity scan approach for net-baryon cumulants"

Phys. Rev. C 109, no.3, 034906 (2024)

J. Brewer et al., Phys. Rev. C 98, 061901 (2018)

Rapidity-dependent yields offers an extra method to explore the EoS at finite chemical potentials.

L.Du, "Bulk medium properties of heavy-ion collisions from the beam energy scan with a multistage hydrodynamic model,"
Phys. Rev. C 110 (2024) no.1, 014904

Thermodynamic properties, especially the baryon chemical potential (μ_B) , undergo significant variations across rapidity,

L.Du, H.Gao, S.Jeon and C.Gale,

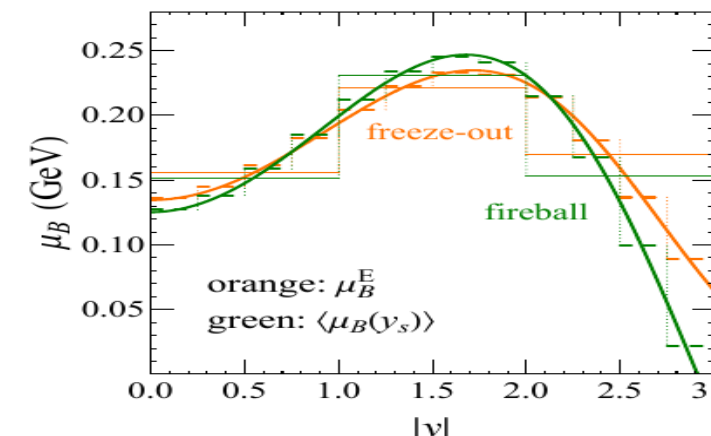
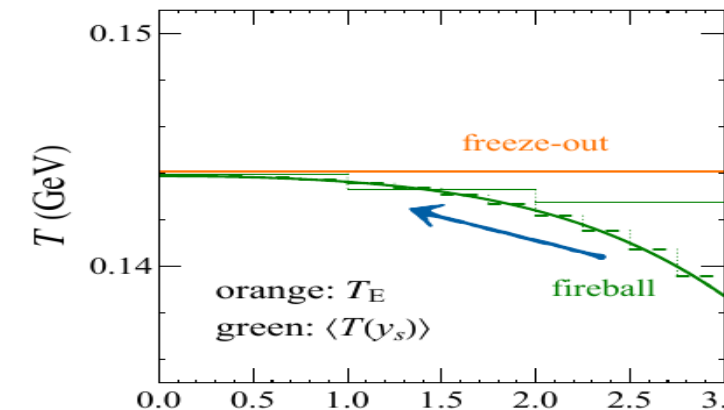
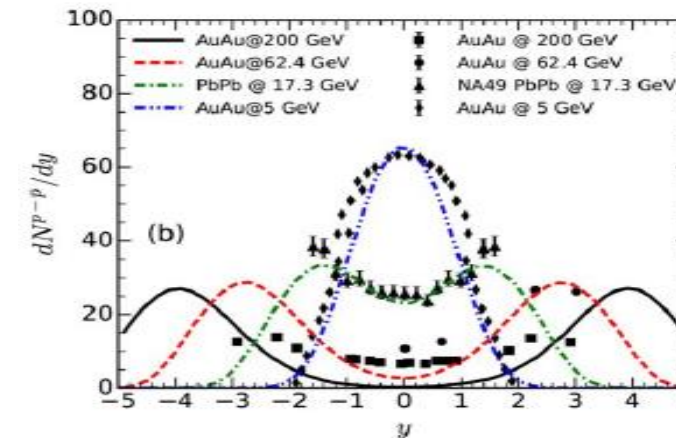
"Rapidity scan with multistage hydrodynamic model,"

Phys. Rev. C 109, no.1, 014907 (2024)

Rapidity dependence of anisotropic flow provides provides sensitivity to (T, μ_B) dependence of specific shear (η/s) and bulk (ζ/s) viscosities

S.A.Jahan, H.Roch and C.Shen,

"Bayesian analysis of (3+1)D relativistic nuclear dynamics with the RHIC data, Phys.Rev.C 110 (2024) 5, 054905



Backup slides